

## Towards stability of radial basis function based cubature formulas\*

Jan Glaubitz<sup>†</sup> and Jonah Reeger<sup>‡</sup>

**Abstract.** Cubature formulas (CFs) based on radial basis functions (RBFs) have become an important tool for multivariate numerical integration of scattered data. Although numerous works have been published on such RBF-CFs, their stability theory can still be considered as underdeveloped. Here, we strive to pave the way towards a more mature stability theory for RBF-CFs. In particular, we prove stability for RBF-CFs based on compactly supported RBFs under certain conditions on the shape parameter and the data points. Moreover, it is shown that asymptotic stability of many RBF-CFs is independent of polynomial terms, which are often included in RBF approximations. While our findings provide some novel conditions for stability of RBF-CFs, the present work also demonstrates that there are still many gaps to fill in future investigations.

**Key words.** Numerical integration, radial basis functions, stability, cardinal functions, discrete orthogonal polynomials

**AMS subject classifications (2020).** 65D30, 65D32, 65D05, 42C05

**1. Introduction.** Numerical integration is an omnipresent task in mathematics and myriad applications. While these are too numerous to list fully, prominent examples include numerical differential equations [47, 75, 1], machine learning [68], finance [36], and biology [63]. In many cases, the problem can be formulated as follows. Let  $\Omega \subset \mathbb{R}^D$  be a bounded domain with positive volume,  $|\Omega| > 0$ . Given  $N$  distinct data pairs  $\{(\mathbf{x}_n, f_n)\}_{n=1}^N \subset \Omega \times \mathbb{R}$  with  $f : \Omega \rightarrow \mathbb{R}$  and  $f_n := f(\mathbf{x}_n)$ , the aim is to approximate the weighted integral

$$(1.1) \quad I[f] := \int_{\Omega} f(\mathbf{x})\omega(\mathbf{x}) \, d\mathbf{x}$$

by an  $N$ -point CF. That is, by a weighted finite sum over the given function of the form

$$(1.2) \quad C_N[f] = \sum_{n=1}^N w_n f(\mathbf{x}_n).$$

Here, the distinct points  $\{\mathbf{x}_n\}_{n=1}^N$  are called *data points* and the  $\{w_n\}_{n=1}^N$  are referred to as *cubature weights*. Many CFs are derived based on the idea to first approximate the (unknown) function  $f$  and to exactly integrate this approximation then [44, 87, 23, 14, 57, 15, 58, 17, 9, 88].

---

\*August 17, 2021

**Corresponding author:** Jan Glaubitz ([Jan.Glaubitz@Dartmouth.edu](mailto:Jan.Glaubitz@Dartmouth.edu), [orcid.org/0000-0002-3434-5563](https://orcid.org/0000-0002-3434-5563))

**Funding:** This work was partially supported by AFOSR #F9550-18-1-0316 and ONR #N00014-20-1-2595 (Glaubitz).

**Disclaimer:** The views expressed in this academic research paper are those of the authors and do not reflect the official policy or position of the United States Government or Department of Defense. In accordance with the Air Force Instruction 51-303, it is not copyrighted, but is the property of the United States government.

<sup>†</sup>Department of Mathematics, Dartmouth College, Hanover, NH 03755, USA

<sup>‡</sup>Senior Research Mathematician, Sensors Directorate, Air Force Research Laboratory, Wright–Patterson Air Force Base, OH 45433, USA

Arguably, most of the existing CFs have been derived to be exact for polynomials up to a certain degree. See [64, 69, 16, 70, 15, 89], in addition to the above references.

That said, in recent years CFs based on the exact integration of RBFs have received a growing amount of interest [86, 84, 83, 74, 2, 34, 76, 78, 91, 77, 85]. The increased use of RBFs for numerical integration, as well as numerical differential equations [56, 54, 24, 55, 60, 52, 82, 30, 27, 42, 43], seems to be only logical, considering their story of success in the last few decades. In fact, since their introduction in Hardy’s work [46] on cartography in 1971, RBFs have become a powerful tool in numerical analysis, including multivariate interpolation and approximation theory [11, 12, 93, 25, 53, 29].

Even though RBF-CFs have been proposed and applied in numerous works by now, their stability theory can still be considered as under-developed, especially when compared to more traditional—e.g. polynomial based—methods. Stability of RBF-CFs was broached, for instance, in [86, 84, 74]. However, to the best of our knowledge, an exhaustive stability theory for RBF-CFs is still missing in the literature. In particular, theoretical results providing clear conditions—e.g., on the kernel, the data points, the weight function, the degree of potentially added polynomial terms—under which stability of RBF-CFs is ensured are rarely encountered.

**1.1. Our Contribution.** The present work strives to at least partially fill this gap in the RBF literature. This is done by providing a detailed theoretical and numerical investigation on stability of RBF-CFs for different families of kernels. These include, compactly supported and Gaussian RBFs as well as polyharmonic splines (PHS).

In particular, we report on the following findings. (1) Stability of RBF-CFs is connected to the Lebesgue constant of the underlying RBF interpolant. Consequently, it is demonstrated that a low stability measure for RBF-CFs is promoted by a low Lebesgue constant. That said, it is also shown that in many cases RBF-CFs have significantly better stability properties than one might expect based on the underlying RBF interpolant. (2) We provide a provable sufficient condition for compactly supported RBFs to yield stable RBF-CF (see [Theorem 5.1](#) in [section 5](#)). The result is independent of the degree of the polynomial term that is included in the RBF interpolant and assumes the data points to come from an equidistributed (space-filling) sequence. This result is obtained by leveraging a beautiful connection to discrete orthogonal polynomials and is partially motivated by arguments that frequently occur in least-squares quadrature/cubature formulas [49, 66, 39]. (3) At least numerically, we find the aforementioned sufficient condition to also be close to necessary in many cases. This might be considered as a discouraging result for compactly supported RBF-CFs since the sufficient condition makes some harsh restrictions on the shape parameter. (4) Finally, the asymptotic stability of pure RBF-CFs is connected to the asymptotic stability of the same RBF-CF but augmented with polynomials of a fixed arbitrary degree. Essentially, we are able to show that for a sufficiently large number of data points, stability of RBF-CFs is independent of the presence of polynomials in the RBF interpolant.

While there are certainly further stability results desired, in addition to the ones presented here, we believe this work to be a valuable step towards a more mature stability theory for RBF-CFs.

**1.2. Outline.** The rest of this work is organized as follows. We start by collecting some preliminaries on RBF interpolants and CFs in [section 2](#). In [section 3](#) a few initial comments

on stability of (RBF-)CFs are offered. Building up on these, it is demonstrated in [section 4](#) that RBF-CFs in many cases have superior stability properties compared to RBF interpolation. Next, [section 5](#) contains our theoretical main result regarding stability of RBF-CFs based on compactly supported kernels. Furthermore, in [section 6](#) it is proven that, under certain assumptions, asymptotic stability of RBF-CFs is independent of the polynomial terms that might be included in the RBF interpolant. The aforementioned theoretical findings are accompanied by various numerical tests in [section 7](#). Finally, concluding thoughts are offered in [section 8](#).

**2. Preliminaries.** We start by collecting some preliminaries on RBF interpolants ([subsection 2.1](#)) as well as RBF-CFs ([subsection 2.2](#)).

**2.1. Radial Basis Function Interpolation.** RBFs are often considered a powerful tool in numerical analysis, including multivariate interpolation and approximation theory [[11](#), [12](#), [93](#), [25](#), [53](#), [29](#)]. In the context of the present work, we are especially interested in RBF interpolants. Let  $f : \mathbb{R}^D \supset \Omega \rightarrow \mathbb{R}$  be a scalar valued function. Given a set of distinct *data points* (in context of RBFs sometimes also referred to as *centers*), the *RBF interpolant* of  $f$  is of the form

$$(2.1) \quad (s_{N,d}f)(\mathbf{x}) = \sum_{n=1}^N \alpha_n \varphi(\varepsilon_n \|\mathbf{x} - \mathbf{x}_n\|_2) + \sum_{k=1}^K \beta_k p_k(\mathbf{x}).$$

Here,  $\varphi : \mathbb{R}_0^+ \rightarrow \mathbb{R}$  is the *RBF* (also called *kernel*),  $\{p_k\}_{k=1}^K$  is a basis of the space of all algebraic polynomials up to degree  $d$ ,  $\mathbb{P}_d(\Omega)$ , and the  $\varepsilon_n$ 's are nonnegative shape parameters. Furthermore, the RBF interpolant [\(2.1\)](#) is uniquely determined by the conditions

$$(2.2) \quad (s_{N,d}f)(\mathbf{x}_n) = f(\mathbf{x}_n), \quad n = 1, \dots, N,$$

$$(2.3) \quad \sum_{n=1}^N \alpha_n p_k(\mathbf{x}_n) = 0, \quad k = 1, \dots, K.$$

In this work, we shall focus on the popular choices of RBFs listed in [Table 1](#). A more complete list of RBFs and their properties can be found in the monographs [[12](#), [93](#), [25](#), [29](#)] and references therein.

*Remark 2.1 (Implementation of  $\varphi(r) = r^{2k} \log r$ ).* The polyharmonic splines (PHS) of the form  $\varphi(r) = r^{2k} \log r$  are usually implemented as  $\varphi(r) = r^{2k-1} \log(r^r)$  to avoid numerical problems at  $r = 0$ , where " $\log(0) = -\infty$ ".

Note that [\(2.2\)](#) and [\(2.3\)](#) can be reformulated as a linear system for the coefficient vectors  $\boldsymbol{\alpha} = [\alpha_1, \dots, \alpha_N]^T$  and  $\boldsymbol{\beta} = [\beta_1, \dots, \beta_K]^T$ . This linear system is given by

$$(2.4) \quad \begin{bmatrix} \Phi & P \\ P^T & 0 \end{bmatrix} \begin{bmatrix} \boldsymbol{\alpha} \\ \boldsymbol{\beta} \end{bmatrix} = \begin{bmatrix} \mathbf{f} \\ \mathbf{0} \end{bmatrix}$$

RBF	$\varphi(r)$	parameter	order
Gaussian	$\exp(-(\varepsilon r)^2)$	$\varepsilon > 0$	0
Wendland's	$\varphi_{D,k}(r)$ , see [92]	$D, k \in \mathbb{N}_0$	0
Polyharmonic splines	$r^{2k-1}$	$k \in \mathbb{N}$	$k$
	$r^{2k} \log r$	$k \in \mathbb{N}$	$k + 1$

Table 1: Some popular RBFs

where  $\mathbf{f} = [f(\mathbf{x}_1), \dots, f(\mathbf{x}_N)]^T$  as well as

$$(2.5) \quad \Phi = \begin{bmatrix} \varphi(\varepsilon_1 \|\mathbf{x}_1 - \mathbf{x}_1\|_2) & \dots & \varphi(\varepsilon_N \|\mathbf{x}_1 - \mathbf{x}_N\|_2) \\ \vdots & & \vdots \\ \varphi(\varepsilon_1 \|\mathbf{x}_N - \mathbf{x}_1\|_2) & \dots & \varphi(\varepsilon_N \|\mathbf{x}_N - \mathbf{x}_N\|_2) \end{bmatrix}, \quad P = \begin{bmatrix} p_1(\mathbf{x}_1) & \dots & p_K(\mathbf{x}_1) \\ \vdots & & \vdots \\ p_1(\mathbf{x}_N) & \dots & p_K(\mathbf{x}_N) \end{bmatrix}.$$

It is well-known that (2.4) is ensured to have a unique solution—corresponding to existence and uniqueness of the RBF interpolant—if the kernel  $\varphi$  is positive definite of order  $m$  and the set of data points is  $\mathbb{P}_m(\Omega)$ -unisolvant. See, for instance, [25, Chapter 7] and [37, Chapter 3.1] or references therein. The set of all RBF interpolants (2.1) forms an  $N$ -dimensional linear space, denote by  $\mathcal{S}_{N,d}$ . This space is spanned by the basis elements

$$(2.6) \quad c_m(\mathbf{x}) = \sum_{n=1}^N \alpha_n^{(m)} \varphi(\varepsilon_n \|\mathbf{x} - \mathbf{x}_n\|_2) + \sum_{k=1}^K \beta_k^{(m)} p_k(\mathbf{x}), \quad m = 1, \dots, N,$$

that are uniquely determined by

$$(2.7) \quad c_m(\mathbf{x}_n) = \delta_{mn} := \begin{cases} 1 & \text{if } m = n, \\ 0 & \text{otherwise,} \end{cases} \quad m, n = 1, \dots, N,$$

and condition (2.3). The functions  $c_m$  are the so-called *cardinal functions*. They provide us with the following representation of the RBF interpolant (2.1):

$$(2.8) \quad (s_{N,d})f(\mathbf{x}) = \sum_{n=1}^N f(\mathbf{x}_n) c_n(\mathbf{x})$$

This representation is convenient to subsequently derive cubature weights based on RBFs that are independent of the function  $f$ .

**2.2. Cubature Formulas Based on Radial Basis Functions.** A fundamental idea behind many CFs is to first approximate the (unknown) functions  $f : \Omega \rightarrow \mathbb{R}$  based on the given data pairs  $\{\mathbf{x}_n, f_n\}_{n=1}^N \subset \Omega \times \mathbb{R}$  and to exactly integrate this approximation. In the case of RBF-CFs this approximation is chosen as the RBF interpolant (2.1). Hence, the corresponding RBF-CF is defined as

$$(2.9) \quad C_N[f] := I[s_{N,d}f] = \int_{\Omega} (s_{N,d}f)(\mathbf{x}) \omega(\mathbf{x}) \, d\mathbf{x}.$$

When formulated w. r. t. the cardinal functions  $c_n$ ,  $n = 1, \dots, N$ , we get

$$(2.10) \quad C_N[f] = \sum_{n=1}^N w_n f(x_n) \quad \text{with} \quad w_n = I[c_n].$$

That is, the RBF cubature weights  $\mathbf{w}$  are given by the moments corresponding to the cardinal functions. This formulation is often preferred over (2.9) since the cubature weights  $\mathbf{w}$  do not have to be recomputed when another function is considered. In our implementation, we compute the RBF cubature weights by solving the linear system

$$(2.11) \quad \underbrace{\begin{bmatrix} \Phi & P \\ P^T & 0 \end{bmatrix}}_{=A} \begin{bmatrix} \mathbf{w} \\ \mathbf{v} \end{bmatrix} = \begin{bmatrix} \mathbf{m}^{\text{RBF}} \\ \mathbf{m}^{\text{poly}} \end{bmatrix},$$

where  $\mathbf{v} \in \mathbb{R}^K$  is an auxiliary vector. Furthermore, the vectors  $\mathbf{m}^{\text{RBF}} \in \mathbb{R}^N$  and  $\mathbf{m}^{\text{poly}} \in \mathbb{R}^K$  contain the moments of the translated kernels and polynomial basis functions, respectively. That is,

$$(2.12) \quad \begin{aligned} \mathbf{m}^{\text{RBF}} &= [I[\varphi_1], \dots, I[\varphi_N]]^T, \\ \mathbf{m}^{\text{poly}} &= [I[p_1], \dots, I[p_K]]^T, \end{aligned}$$

with  $\varphi_n(\mathbf{x}) = \varphi(\varepsilon_n \|\mathbf{x} - \mathbf{x}_n\|_2)$ . The moments of different RBFs can be found in [Appendix A](#) and references listed there. The moments of polynomials for different domains  $\Omega$  can be found in the literature, e. g., [\[38, Appendix A\]](#) and [\[28, 62\]](#).

**3. Stability and the Lebesgue Constant.** In this section, we address stability of RBF interpolants and the corresponding RBF-CFs. In particular, we show that both can be estimated in terms of the famous Lebesgue constant. That said, we also demonstrate that RBF-CFs often come with improved stability compared to RBF interpolation.

**3.1. Stability and Accuracy of Cubature Formulas.** We start by addressing stability and accuracy of RBF-CFs. To this end, let us denote the best approximation of  $f$  from  $\mathcal{S}_{N,d}$  in the  $L^\infty$ -norm by  $\hat{s}$ . That is,

$$(3.1) \quad \hat{s} = \arg \min_{s \in \mathcal{S}_{N,d}} \|f - s\|_{L^\infty(\Omega)} \quad \text{with} \quad \|f - s\|_{L^\infty(\Omega)} = \sup_{\mathbf{x} \in \Omega} |f(\mathbf{x}) - s(\mathbf{x})|.$$

Note that this best approximation w. r. t. the  $L^\infty$ -norm is not necessarily equal to the RBF interpolant. Still, the following error bound holds for the RBF-CF (2.10), that corresponds to exactly integrating the RBF interpolant from  $\mathcal{S}_{N,d}$ :

$$(3.2) \quad |C_N[f] - I[f]| \leq (\|I\|_\infty + \|C_N\|_\infty) \inf_{s \in \mathcal{S}_{N,d}} \|f - s\|_{L^\infty(\Omega)}$$

Inequality (3.2) is commonly known as the Lebesgue inequality; see, e. g., [\[90\]](#) or [\[9, Theorem 3.1.1\]](#). It is most often encountered in the context of polynomial interpolation [\[10, 50\]](#), but

straightforwardly carries over to numerical integration. In this context, the operator norms  $\|I\|_\infty$  and  $\|C_N\|_\infty$  are respectively given by  $\|I\|_\infty = I[1]$  and

$$(3.3) \quad \|C_N\|_\infty = \sum_{n=1}^N |w_n| = \sum_{n=1}^N |I[c_n]|.$$

Recall that the  $c_n$ 's are the cardinal functions (see [subsection 2.1](#)).

In fact,  $\|C_N\|_\infty$  is a common stability measure for CFs. This is because the propagation of input errors, e. g., due to noise or rounding errors, can be bounded as follows:

$$(3.4) \quad |C_N[f] - C_N[\tilde{f}]| \leq \|C_N\|_\infty \|f - \tilde{f}\|_{L^\infty}$$

That is, input errors are amplified at most by a factor that is equal to the operator norm  $\|C_N\|_\infty$ . At the same time, we have a lower bound for  $\|C_N\|_\infty$  given by

$$(3.5) \quad \|C_N\|_\infty \geq C_N[1],$$

where equality holds if and only if all cubature weights are nonnegative. This is the reason for which the construction of CFs is mainly devoted to nonnegative CFs.

**Definition 3.1 (Stability).** *We call the RBF-CF  $C_N$  stable if  $\|C_N\|_\infty = C_N[1]$  holds. This is the case if and only if  $I[c_n] \geq 0$  for all cardinal functions  $c_n$ ,  $n = 1, \dots, N$ .*

It is also worth noting that  $C[1] = \|I\|_\infty$  if the CF is exact for constants. For RBF-CFs, this is the case if at least constants are included in the underlying RBF interpolant ( $d \geq 0$ ).

Summarizing the above discussion originating from the Lebesgue inequality [\(3.2\)](#), we have a two-fold goal when using RBF-CFs. On the one hand, the data points, the kernel, the shape parameter, and the basis of polynomials should be chosen such that  $\mathcal{S}_{N,d}$  provides a best approximation to  $f$  in the  $L^\infty$ -norm that is as accurate as possible. On the other hand, to ensure stability,  $\|C_N\|_\infty$  should be as small as possible. That is,  $I[c_n] \geq 0$  for all cardinal functions  $c_n \in \mathcal{S}_{N,d}$ .

**3.2. Stability of RBF Approximations.** We now demonstrate how the stability of RBF-CFs can be connected to the stability of the corresponding RBF interpolant. Indeed, the stability measure  $\|C_N\|_\infty$  can be bounded from above by

$$(3.6) \quad \|C_N\|_\infty \leq \|I\|_\infty \Lambda_N, \quad \text{with} \quad \Lambda_N := \sup_{\mathbf{x} \in \Omega} \sum_{n=1}^N |c_n(\mathbf{x})|.$$

Here,  $\Lambda_N$  is the Lebesgue constant corresponding to the recovery process  $f \mapsto s_{N,d}f$  (RBF interpolation). Obviously,  $\Lambda_N \geq 1$ . Note that if  $1 \in \mathcal{S}_{N,d}$  (the RBF-CF is exact for constants), we therefore have

$$(3.7) \quad \|I\|_\infty \leq \|C_N\|_\infty \leq \|I\|_\infty \Lambda_N.$$

Hence, the RBF-CF is stable ( $\|C_N\|_\infty = \|I\|_\infty$ ) if  $\Lambda_N$  is minimal ( $\Lambda_N = 1$ ). We briefly note that the inequality  $\|C_N\|_\infty \leq \|I\|_\infty \Lambda_N$  is sharp by considering the following [Example 3.2](#).

*Example 3.2* ( $\|C_N\|_\infty = \Lambda_N$ ). Let us consider the one-dimensional domain  $\Omega = [0, 1]$  with  $\omega \equiv 1$ , which immediately implies  $\|I\|_\infty = 1$ . In [6] it was shown that for the linear PHS  $\varphi(r) = r$  and data points  $0 = x_1 < x_2 < \dots < x_N = 1$  the corresponding cardinal functions  $c_m$  are simple hat functions. In particular,  $c_m$  is the ordinary “connect the dots” piecewise linear interpolant of the data pairs  $(x_n, \delta_{nm})$ ,  $n = 1, \dots, N$ . Thus,  $\Lambda_N = 1$ . At the same time, this yields  $\|C_N\|_\infty = 1$  and therefore  $\|C_N\|_\infty = \Lambda_N$ .

Looking for minimal Lebesgue constants is a classical problem in recovery theory. For instance, it is well known that for polynomial interpolation even near-optimal sets of data points yield a Lebesgue constant that grows as  $\mathcal{O}(\log N)$  in one dimension and as  $\mathcal{O}(\log^2 N)$  in two dimensions; see [10, 5, 7, 50] and references therein. In the case of RBF interpolation, the Lebesgue constant and appropriate data point distributions were studied in [51, 18, 65, 20] and many more works. That said, the second inequality in (3.7) also tells us that in some cases we can expect the RBF-CF to have superior stability properties compared to the underlying RBF interpolant. In fact, this might not come as a surprise since integration is well-known to have a smoothing (stabilizing) effect in a variety of different contexts. Finally, it should be stressed that (3.7) only holds if  $1 \in \mathcal{S}_{N,d}$ . In general,

$$(3.8) \quad C_N[1] \leq \|C_N\|_\infty \leq \|I\|_\infty \Lambda_N.$$

Still, this indicates that a recovery space  $\mathcal{S}_{N,d}$  is desired that yields a small Lebesgue constant as well as the RBF-CF potentially having superior stability compared to RBF interpolation.

**4. Theoretical Stability, Numerical Conditioning, and Robustness.** In this section, we report on two important observations. The first being that in many cases we find RBF-CFs to have superior stability properties compared to the corresponding RBF interpolants. That is, we show that most often a strict inequality,  $\|C_N\|_\infty < \|I\|_\infty \Lambda_N$ , holds for the second inequality in (3.7). Second, we emphasize the importance to distinguish between *theoretical stability* (the CF having nonnegative weights only) and overall *robustness* of the CF. The latter one is not just influenced by the theoretical stability—assuming infinite arithmetics—but also incorporates the effect of numerical conditioning. In particular, the cubature weights  $\mathbf{w}$  are computed by numerically solving the linear system (2.11). On a computer, this is always done in some finite arithmetic which inevitably results in rounding errors. Such rounding errors can also propagate into the cubature weights  $\mathbf{w}$  and, depending on the conditioning of the coefficient matrix  $A$ , might cause the RBF-CF to decrease in robustness. That said, our findings below indicate that despite the matrix  $A$  often having potentially prohibitively high condition numbers, the numerical computation of the cubature weights  $\mathbf{w}$  still yields accurate results for these. Henceforth, for sake of simplicity, we assume  $\omega \equiv 1$ .

We start by demonstrating that RBF-CFs in many cases can have superior stability properties compared to RBF interpolants. This is demonstrated in Figure 1 for  $\Omega = [0, 1]$  and a Gaussian kernel  $\varphi(r) = \exp(-\varepsilon^2 r^2)$ . The corresponding RBF approximation was either augmented with no polynomial terms (Figure 1a), a constant term (Figure 1b), or a linear term (Figure 1c). See the caption of Figure 1 for more details. The following observations can be made based on the results presented in Figure 1: (1) RBF-based integration can be distinctly more stable than RBF-based interpolation. This is indicated by the stability measure  $\|C_N\|_\infty$



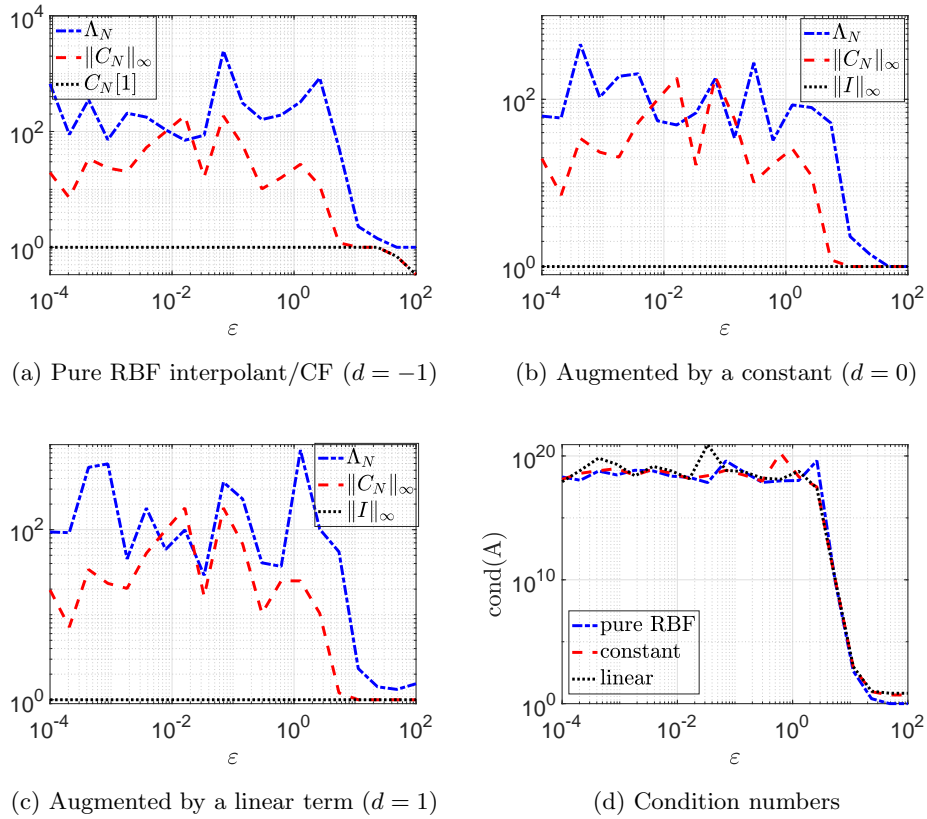


Figure 1: A comparison of the stability measure  $\|C_N\|_\infty$ , the Lebesgue constant  $\Lambda_N$ , and the condition number  $\text{cond}(A)$  for the Gaussian kernel.  $N = 20$  equidistant data points were considered, while the shape parameter  $\varepsilon$  was allowed to vary. Note that for the pure RBF interpolant/CF ( $d = -1$ ), the optimal stability measure is  $C_N[1]$  rather than  $\|I\|_\infty = 1$ .

often being smaller than the Lebesgue constant  $\Lambda_N$ . (2) Finding stable (nonnegative) RBF-CFs is a nontrivial task. Even though, in the tests presented here, we can observe certain regions of stability w. r. t. the shape parameter  $\varepsilon$ , it is not clear how to theoretically quantify the boundary of this region. A first step towards such an analysis is presented in [section 5](#) for compactly supported RBFs. Further results in this direction would be of great interest. (3) There are two potential sources for negative weights, causing  $\|C_N\|_\infty > C_N[1]$  and the RBF-CF to become sensitive towards input errors. On one hand, this can be caused by one (or multiple) of the cardinal functions having a negative moment. This is what we previously referred to as “theoretical instability”. On the other hand, negative weights might also be caused by numerical ill-conditioning by the coefficient matrix  $A$  in the linear system (2.11) that is numerically solved to compute the cubature weights. In fact, we can observe such numerical ill-conditioning in [Figure 1a](#) and [Figure 1b](#). In these figures, we have  $\|C_N\|_\infty > \|I\|_\infty \Lambda_N$  (note that  $\|I\|_\infty = 1$ ) for  $\varepsilon \approx 10^{-2}$ . Theoretically—assuming error-free computations—this should



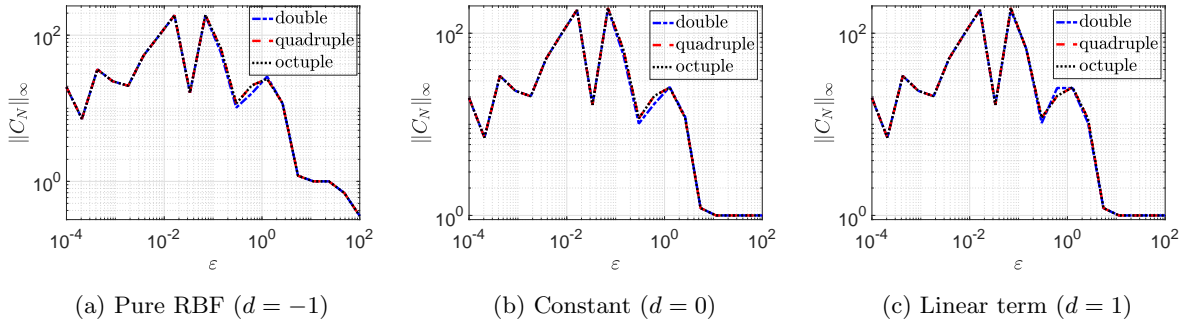


Figure 2: Comparison of the stability measure  $\|C_N\|_\infty$  for different computational precisions. Considered are double (32 bits), quadruple (64 bits) and octuple (128 bits) precision. In all cases  $N = 20$  equidistant data points and the Gaussian kernel were used. The corresponding RBF interpolant either included no polynomial terms ( $d = -1$ ), a constant ( $d = 0$ ) or a linear ( $d = 1$ ) term.

not happen. In accordance with this, [Figure 1d](#) illustrates that in all cases ( $d = -1, 0, 1$ ) the condition number of the matrix  $A$ ,  $\text{cond}(A)$ , reaches the upper bound of (decimal) double precision arithmetics ( $\approx 10^{16}$ ) for  $\varepsilon$  close to  $10^0$ .

*Remark 4.1 (The Uncertainty Principle for Direct RBF Methods).* Severe ill-conditioning of  $A$  for flat RBFs (small shape parameters  $\varepsilon$ ) is a well-known phenomenon in the RBF community. At the same time, one often finds that the best accuracy for an RBF interpolant is achieved when  $\varepsilon$  is small. This so-called *uncertainty* or *trade-off principle* of (direct) RBF methods was first formulated in [80]. Unfortunately, it has contributed to a widespread misconception that numerical ill-conditioning is unavoidable for flat RBFs. It should be stressed that the uncertainty principle is specific to the direct RBF approach [22, 33, 61, 81]. That is, when  $A$  is formulated w. r. t. the basis consisting of the translated RBFs, as described in (2.5). Indeed, by now, numerous works have demonstrated that severe ill-conditioning of  $A$  for flat RBFs can be remedied by formulating  $A$  and the linear system (2.11) w. r. t. to certain more stable bases spanning the RBF space  $\mathcal{S}_{N,d}$ . See [67, 73, 31, 26, 19, 32, 95] and references therein. However, it should be noted that the linear system (2.11) used to determine the cubature weights of the RBF-CF requires knowledge of the moments of the basis that is used to formulate  $A$ . This might be a potential bottleneck for some of the above-listed approaches. A detailed discussion of how the moments of stable bases of  $\mathcal{S}_{N,d}$  can be determined would therefore be of interest.

The results presented in [Figure 1](#) were obtained by the direct RBF method. One may therefore wonder to which extent the observed instabilities are influenced by numerical ill-conditioning. To address this question, we have repeated the same test with an increased computational precision using the function *vpa* in MATLAB. [Figure 2](#) provides a comparison of the stability measure  $\|C_N\|_\infty$  computed by double (32 bits), quadruple (64 bits) and octuple (128 bits) precision. Despite  $A$  being highly ill-conditioned, the results for quadruple precision might be considered as “close” to the ones for usual double precision. In addition, further

increasing the precision from quadruple to octuple precision does not seem to change the results—at least not by the naked eye. These results agree with the often reported observation that using stable solvers leads to useful results and well-behaved RBF interpolants even in the case of unreasonably large condition numbers. Indeed, we observe that the observed instabilities for RBF-CFs cannot be explained by numerical ill-conditioning alone. Rather, our results indicate that numerical ill-conditioning only amplifies already existing (theoretical) instabilities in the RBF-CF.

**5. Compactly Supported Radial Basis Functions.** There is a rich body of literature on stability results for CFs based on (algebraic and trigonometric) polynomials, including [44, 87, 8, 23, 14, 57, 58, 17, 9] and the many references therein. In comparison, provable results on the stability of RBF-CFs are rarely encountered in the literature, despite their increased use in applications. Here, our goal is to pave the way towards a more mature stability theory for these. As a first step in this direction, we next prove stability of RBF-CFs for compactly supported kernels with nonoverlapping supports. To be more precise, we subsequently consider RBFs  $\varphi : \mathbb{R}_0^+ \rightarrow \mathbb{R}$  satisfying the following restrictions:

(R1)  $\varphi$  is nonnegative, i. e.,  $\varphi \geq 0$ .

(R2)  $\varphi$  is uniformly bounded. W.l.o.g. we assume  $\max_{r \in \mathbb{R}_0^+} |\varphi(r)| = 1$ .

(R3)  $\varphi$  is compactly supported. W.l.o.g. we assume  $\text{supp } \varphi = [0, 1]$ .

Already note that (R3) implies  $\text{supp } \varphi_n = B_{\varepsilon_n^{-1}}(\mathbf{x}_n)$ , where

$$(5.1) \quad B_{\varepsilon_n^{-1}}(\mathbf{x}_n) := \{ \mathbf{x} \in \Omega \mid \|\mathbf{x}_n - \mathbf{x}\|_2 \leq \varepsilon_n^{-1} \}, \quad \varphi_n(\mathbf{x}) := \varphi(\varepsilon_n \|\mathbf{x}_n - \mathbf{x}\|_2).$$

Clearly, the  $\varphi_n$ 's will have nonoverlapping support if the shape parameters  $\varepsilon_n$  are sufficiently large. This can be ensured by the following condition:

$$(5.2) \quad \varepsilon_n^{-1} \leq h_n := \min \{ \|\mathbf{x}_n - \mathbf{x}_m\|_2 \mid \mathbf{x}_m \in X \setminus \{\mathbf{x}_n\} \}, \quad n = 1, \dots, N$$

Here,  $X$  denotes the set of data points. The different basis functions having nonoverlapping support might seem to be a fairly restrictive sufficient condition. However, our numerical tests presented in section 7 indicate that this condition does not seem to be “far away” from being necessary as well. This might be considered as a discouraging result for the utility of compactly supported RBFs in the context of numerical integration. Finally, it should be pointed out that throughout this section, we assume  $\omega \equiv 1$ . This assumption is made for the main result, Theorem 5.1, to hold. Its role will become clearer after consulting the proof of Theorem 5.1 and is revisited in Remark 5.6.

**5.1. Main Results.** Our main result is the following Theorem 5.1. It states that RBF-CFs are conditionally stable for any polynomial degree  $d \in \mathbb{N}$  if the number of (equidistributed) data points,  $N$ , is sufficiently larger than  $d$ .

**Theorem 5.1 (Conditional Stability of RBF-CFs).** *Let  $(\mathbf{x}_n)_{n \in \mathbb{N}}$  be an equidistributed sequence in  $\Omega$  and  $X_N = \{\mathbf{x}_n\}_{n=1}^N$ . Furthermore, let  $\omega \equiv 1$ , let  $\varphi : \mathbb{R}_0^+ \rightarrow \mathbb{R}$  be a RBF satisfying (R1) to (R3), and choose the shape parameters  $\varepsilon_n$  such that the corresponding functions  $\varphi_n$  have nonoverlapping support and equal moments ( $I[\varphi_n] = I[\varphi_m]$  for all  $n, m = 1, \dots, N$ ). For every polynomial degree  $d \in \mathbb{N}$  there exists an  $N_0 \in \mathbb{N}$  such that for all  $N \geq N_0$  the corresponding RBF-CF (2.10) is stable. That is,  $I[c_m] \geq 0$  for all  $m = 1, \dots, N$ .*

The proof of [Theorem 5.1](#) is given in [subsection 5.4](#) after collecting a few preliminary results.

Note that a sequence  $(\mathbf{x}_n)_{n \in \mathbb{N}}$  is *equidistributed in  $\Omega$*  if and only if

$$(5.3) \quad \lim_{N \rightarrow \infty} \frac{|\Omega|}{N} \sum_{n=1}^N g(\mathbf{x}_n) = \int_{\Omega} g(\mathbf{x}) \, d\mathbf{x}$$

holds for all measurable bounded functions  $g : \Omega \rightarrow \mathbb{R}$  that are continuous almost everywhere (in the sense of Lebesgue), see [\[94\]](#). For details on equidistributed sequences, we refer to the monograph [\[59\]](#). Still, it should be noted that equidistributed sequences are dense sequences with a special ordering. In particular, if  $(\mathbf{x}_n)_{n \in \mathbb{N}} \subset \Omega$  is equidistributed, then for every  $d \in \mathbb{N}$  there exists an  $N_0 \in \mathbb{N}$  such that  $X_N$  is  $\mathbb{P}_d(\Omega)$ -unisolvent for all  $N \geq N_0$ ; see [\[40\]](#). This ensures that the corresponding RBF interpolant is well-defined.

It should also be noted that if  $\Omega \subset \mathbb{R}^D$  is bounded and has a boundary of measure zero (again in the sense of Lebesgue), then an equidistributed sequence in  $\Omega$  is induced by every equidistributed sequence in the  $D$ -dimensional hypercube. Since  $\Omega$  is bounded, we can find an  $R > 0$  such that  $\Omega \subset [-R, R]^D$ . Let  $(\mathbf{y}_n)_{n \in \mathbb{N}}$  be an equidistributed sequence in  $[-R, R]^D$ .<sup>1</sup> Next, define  $(\mathbf{x}_n)_{n \in \mathbb{N}}$  as the subsequence of  $(\mathbf{y}_n)_{n \in \mathbb{N}} \subset [-R, R]^D$  that only contains the points inside of  $\Omega$ . It was shown in [\[40\]](#) that this results in  $(\mathbf{x}_n)_{n \in \mathbb{N}}$  being equidistributed in  $\Omega$  if  $\partial\Omega$  is of measure zero.

**5.2. Explicit Representation of the Cardinal Functions.** In preparation of proving [Theorem 5.1](#) we derive an explicit representation for the cardinal functions  $c_n$  under the restrictions [\(R1\)](#) to [\(R3\)](#) and [\(5.2\)](#). In particular, we make use of the concept of discrete orthogonal polynomials. Let us define the following discrete inner product corresponding to the data points  $X_N = \{\mathbf{x}_n\}_{n=1}^N$ :

$$(5.4) \quad [u, v]_{X_N} = \frac{|\Omega|}{N} \sum_{n=1}^N u(\mathbf{x}_n) v(\mathbf{x}_n)$$

Recall that the data points  $X_N$  are coming from an equidistributed sequence and are therefore ensured to be  $\mathbb{P}_d(\Omega)$ -unisolvent for any degree  $d \in \mathbb{N}$  if a sufficiently large number of data points is used. In this case, [\(5.4\)](#) is therefore ensured to be positive definite on  $\mathbb{P}_d(\Omega)$ . We say that the basis  $\{p_k\}_{k=1}^K$  of  $\mathbb{P}_d(\Omega)$ , where  $K = \dim \mathbb{P}_d(\Omega)$ , consists of *discrete orthogonal polynomials (DOPs)* if they satisfy

$$(5.5) \quad [p_k, p_l]_{X_N} = \delta_{kl} := \begin{cases} 1 & \text{if } k = l, \\ 0 & \text{otherwise,} \end{cases} \quad k, l = 1, \dots, K.$$

We now come to the desired explicit representation for the cardinal functions  $c_m$ .

**Lemma 5.2 (Explicit Representation for  $c_m$ ).** *Let the RBF  $\varphi : \mathbb{R}_0^+ \rightarrow \mathbb{R}$  satisfy [\(R2\)](#) and [\(R3\)](#). Furthermore, choose the shape parameters  $\varepsilon_n$  such that the corresponding functions  $\varphi_n$*

---

<sup>1</sup>Examples for such sequences include certain equidistant, (scaled and translated) Halton [\[45\]](#) or some other low-discrepancy points [\[48, 71, 13, 21\]](#).

have nonoverlapping support and let the basis  $\{p_k\}_{k=1}^K$  consists of DOPs. Then, the cardinal function  $c_m$ ,  $m = 1, \dots, N$ , is given by

$$(5.6) \quad c_m(\mathbf{x}) = \varphi_m(\mathbf{x}) - \frac{|\Omega|}{N} \sum_{n=1}^N \left( \sum_{k=1}^K p_k(\mathbf{x}_m) p_k(\mathbf{x}_n) \right) \varphi_n(\mathbf{x}) + \frac{|\Omega|}{N} \sum_{k=1}^K p_k(\mathbf{x}_m) p_k(\mathbf{x}).$$

*Proof.* Let  $m, n \in \{1, \dots, N\}$ . The restrictions (R2), (R3) together with the assumption of the  $\varphi_n$ 's having nonoverlapping support yields  $\varphi_n(\mathbf{x}_m) = \delta_{mn}$ . Hence, (2.6) and (2.7) imply

$$(5.7) \quad \alpha_n^{(m)} = \delta_{mn} - \sum_{k=1}^K \beta_k^{(m)} p_k(\mathbf{x}_n).$$

If we substitute (5.7) into (2.3), we get

$$(5.8) \quad p_l(\mathbf{x}_m) - \frac{N}{|\Omega|} \sum_{k=1}^K \beta_k^{(m)} [p_k, p_l]_{X_N} = 0, \quad l = 1, \dots, K.$$

Thus, if  $\{p_k\}_{k=1}^K$  consists of DOPs, this gives us

$$(5.9) \quad \beta_l^{(m)} = \frac{N}{|\Omega|} p_l(\mathbf{x}_m), \quad l = 1, \dots, K.$$

Finally, substituting (5.9) into (5.7) yields

$$(5.10) \quad \alpha_n^{(m)} = \delta_{mn} - \frac{N}{|\Omega|} \sum_{k=1}^K p_k(\mathbf{x}_m) p_k(\mathbf{x}_n)$$

and therefore the assertion. ■

We already remarked that using a basis consisting of DOPs is not necessary for the implementation of RBF-CFs. In fact, the cubature weights are, ignoring computational considerations, independent of the polynomial basis elements w. r. t. which the matrix  $P$  and the corresponding moments  $\mathbf{m}^{\text{poly}}$  are formulated. We only use DOPs as a theoretical tool—a convenient perspective on the problem at hand<sup>2</sup>—to show stability of RBF-CFs.

**5.3. Some Low Hanging Fruits.** Using the explicit representation (5.6) it is trivial to prove stability of RBF-CFs when no polynomial term or only a constant is included in the RBF interpolant.

**Lemma 5.3 (No Polynomials).** *Let the RBF  $\varphi : \mathbb{R}_0^+ \rightarrow \mathbb{R}$  satisfy (R1) to (R3) and choose the shape parameters  $\varepsilon_n$  such that the corresponding functions  $\varphi_n$  have nonoverlapping support. Assume that no polynomials are included in the corresponding RBF interpolant ( $K = 0$ ). Then, the associated RBF-CF is stable, i.e.,  $I[c_m] \geq 0$  for all  $m = 1, \dots, N$ .*

---

<sup>2</sup>For example, many properties of interpolation polynomials are shown by representing these w. r. t. the Lagrange basis, while this representation is often not recommended for actual computations.

*Proof.* It is obvious that  $c_m(\mathbf{x}) = \varphi_m(\mathbf{x})$ . Thus, by restriction (R1),  $c_m$  is nonnegative and therefore  $I[c_m] \geq 0$ . ■

**Lemma 5.4 (Only a Constant).** *Let the RBF  $\varphi : \mathbb{R}_0^+ \rightarrow \mathbb{R}$  satisfy (R1) to (R3) and choose the shape parameters  $\varepsilon_n$  such that the corresponding functions  $\varphi_n$  have nonoverlapping support. Assume that only a constant is included in the corresponding RBF interpolant ( $d = 0$  or  $K = 1$ ). Then, the associated RBF-CF is stable, i.e.,  $I[c_m] \geq 0$  for all  $m = 1, \dots, N$ .*

*Proof.* Let  $m \in \{1, \dots, N\}$ . If we choose  $p_1 \equiv |\Omega|^{-1/2}$ , Lemma 5.2 yields

$$(5.11) \quad c_m(\mathbf{x}) = \varphi_m(\mathbf{x}) + \frac{1}{N} \left( 1 - \sum_{n=1}^N \varphi_n(\mathbf{x}) \right).$$

Note that by (R2), (R3), and (5.2), we therefore have  $c_m(\mathbf{x}) \geq \varphi_m(\mathbf{x})$ . Hence, (R1) implies the assertion. ■

**5.4. Proof of the Main Results.** The following technical lemma will be convenient to the proof of Theorem 5.1.

**Lemma 5.5.** *Let  $(\mathbf{x}_n)_{n \in \mathbb{N}}$  be equidistributed in  $\Omega$ ,  $X_N = \{\mathbf{x}_n\}_{n=1}^N$ , and let  $[\cdot, \cdot]_{X_N}$  be the discrete inner product (5.4). Furthermore, let  $\{p_k^{(N)}\}_{k=1}^K$  be a basis of  $\mathbb{P}_d(\Omega)$  consisting of DOPs w. r. t.  $[\cdot, \cdot]_{X_N}$ . Then, for all  $k = 1, \dots, K$ ,*

$$(5.12) \quad p_k^{(N)} \rightarrow p_k \quad \text{in } L^\infty(\Omega), \quad N \rightarrow \infty,$$

where  $\{p_k\}_{k=1}^K$  is a basis of  $\mathbb{P}_d(\Omega)$  consisting of continuous orthogonal polynomials satisfying

$$(5.13) \quad \int_{\Omega} p_k(\mathbf{x}) p_l(\mathbf{x}) \, d\mathbf{x} = \delta_{kl}, \quad k, l = 1, \dots, K.$$

Moreover, it holds that

$$(5.14) \quad \lim_{N \rightarrow \infty} \int_{\Omega} p_k^{(N)}(\mathbf{x}) p_l^{(N)}(\mathbf{x}) \, d\mathbf{x} = \delta_{kl}, \quad k, l = 1, \dots, K.$$

*Proof.* The assertion is a direct consequence of the results from [38]. ■

Essentially, Lemma 5.5 states that if a sequence of discrete inner product converges to a continuous one, then also the corresponding DOPs—assuming that the ordering of the elements does not change—converges to a basis of continuous orthogonal polynomials. Furthermore, this convergence also holds in a uniform sense. We are now able to provide a proof for Theorem 5.1.

*Proof of Theorem 5.1.* Let  $d \in \mathbb{N}$  and  $m \in \{1, \dots, N\}$ . Under the assumptions of Theorem 5.1, we have  $I[\varphi_n] = I[\varphi_m]$  for all  $n = 1, \dots, N$ . Thus, Lemma 5.2 implies

$$(5.15) \quad I[c_m] = I[\varphi_m] \left[ 1 - \frac{|\Omega|}{N} \sum_{n=1}^N \sum_{k=1}^K p_k^{(N)}(\mathbf{x}_m) p_k^{(N)}(\mathbf{x}_n) \right] + \frac{|\Omega|}{N} \sum_{k=1}^K p_k^{(N)}(\mathbf{x}_m) I[p_k].$$

Let  $\{p_k^{(N)}\}_{k=1}^K$  be a basis of  $\mathbb{P}_d(\Omega)$  consisting of DOPs. That is,  $[p_k^{(N)}, p_l^{(N)}]_{X_N} = \delta_{kl}$ . In particular,  $p_1^{(N)} \equiv |\Omega|^{-1/2}$ . With this in mind, it is easy to verify that

$$(5.16) \quad \frac{|\Omega|}{N} \sum_{n=1}^N \sum_{k=1}^K p_k^{(N)}(\mathbf{x}_m) p_k^{(N)}(\mathbf{x}_n) = \sum_{k=1}^K p_k^{(N)}(\mathbf{x}_m) |\Omega|^{1/2} [p_k^{(N)}, p_1^{(N)}]_{X_N} = 1.$$

Thus, we have

$$(5.17) \quad I[c_m] \geq 0 \iff \sum_{k=1}^K p_k^{(N)}(\mathbf{x}_m) I[p_k^{(N)}] \geq 0.$$

Finally, observe that

$$(5.18) \quad \sum_{k=1}^K p_k^{(N)}(\mathbf{x}_m) I[p_k^{(N)}] = |\Omega|^{1/2} \sum_{k=1}^K p_k^{(N)}(\mathbf{x}_m) \int_{\Omega} p_k^{(N)}(\mathbf{x}) p_1^{(N)}(\mathbf{x}) d\mathbf{x},$$

under the assumption that  $\omega \equiv 1$ . [Lemma 5.5](#) therefore implies

$$(5.19) \quad \lim_{N \rightarrow \infty} \sum_{k=1}^K p_k^{(N)}(\mathbf{x}_m) I[p_k^{(N)}] = 1,$$

which completes the proof. ■

*Remark 5.6 (On the Assumption that  $\omega \equiv 1$ ).* The assumption that  $\omega \equiv 1$  in [Theorem 5.1](#) is necessary for [\(5.16\)](#) and [\(5.19\)](#) to both hold true. On the one hand, [\(5.16\)](#) is ensured by the the DOPs being orthogonal w. r. t. the discrete inner product [\(5.4\)](#). This discrete inner product can be considered as an approximation to the continuous inner product  $\langle u, v \rangle = \int_{\Omega} u(\mathbf{x})v(\mathbf{x}) d\mathbf{x}$ . This also results in [Lemma 5.5](#). On the other hand, in general, [\(5.19\)](#) only holds if the DOPs converge to a basis of polynomials that is orthogonal w. r. t. the weighted continuous inner product  $\langle u, v \rangle_{\omega} = \int_{\Omega} u(\mathbf{x})v(\mathbf{x})\omega(\mathbf{x}) d\mathbf{x}$ . Hence, for [\(5.16\)](#) and [\(5.19\)](#) to both hold true at the same time, we have to assume that  $\omega \equiv 1$ . In this case, the two continuous inner products are the same.

**6. On the Connection Between RBF-CFs With and Without Polynomials.** A natural question in the context of RBFs is which influence the polynomial terms have on the quality of the RBF interpolation and the RBF-CF, beyond ensuring existence of the RBF interpolant. In particular, in the context of the present work, one might ask “how are polynomial terms influencing stability of the RBF-CF?”. In what follows, we address this question by showing that—under certain assumptions that are to be specified yet—at least asymptotic stability of RBF-CFs is independent of polynomial terms. We hope this result to be another step forward towards a more mature stability theory for RBF-CFs.

Recently, the following explicit formula for the cardinal functions was derived in [\[4, 3\]](#). Let us denote  $\mathbf{c}(\mathbf{x}) = [c_1(\mathbf{x}), \dots, c_N(\mathbf{x})]^T$ , where  $c_1, \dots, c_N$  are the cardinal functions spanning  $\mathcal{S}_{N,d}$ ; see [\(2.6\)](#) and [\(2.7\)](#). Provided that  $\Phi$  and  $P$  in [\(2.5\)](#) have full rank<sup>3</sup>,

$$(6.1) \quad \mathbf{c}(\mathbf{x}) = \hat{\mathbf{c}}(\mathbf{x}) - B\boldsymbol{\tau}(\mathbf{x})$$

---

<sup>3</sup> $P$  having full rank means that  $P$  has full column rank, i. e., the columns of  $P$  are linearly independent. This is equivalent to the set of data points being  $\mathbb{P}_d(\Omega)$ -unisolvant.

holds. Here,  $\hat{\mathbf{c}}(\mathbf{x}) = [\hat{c}_1(\mathbf{x}), \dots, \hat{c}_N(\mathbf{x})]^T$  are the cardinal functions corresponding to the pure RBF interpolation without polynomials. That is, they span  $\mathcal{S}_{N,-1}$ . At the same time,  $B$  and  $\boldsymbol{\tau}$  are defined as

$$(6.2) \quad B := \Phi^{-1}P \left( P^T \Phi^{-1}P \right)^{-1}, \quad \boldsymbol{\tau}(\mathbf{x}) := P^T \hat{\mathbf{c}}(\mathbf{x}) - \mathbf{p}(\mathbf{x})$$

with  $\mathbf{p}(\mathbf{x}) = [p_1(\mathbf{x}), \dots, p_K(\mathbf{x})]^T$ . Note that  $\boldsymbol{\tau}$  can be interpreted as a residual measuring how well pure RBFs can approximate polynomials up to degree  $d$ . Obviously, (6.1) implies

$$(6.3) \quad \mathbf{w} = \hat{\mathbf{w}} - BI[\boldsymbol{\tau}],$$

where  $\mathbf{w}$  is the vector of cubature weights of the RBF-CF with polynomials ( $d \geq 0$ ). At the same time,  $\hat{\mathbf{w}}$  is the vector of weights corresponding to the pure RBF-CF without polynomial augmentation ( $d = -1$ ). Moreover,  $I[\boldsymbol{\tau}]$  denotes the componentwise application of the integral operator  $I$ . It was numerically demonstrated in [4] that for fixed  $d \in \mathbb{N}$

$$(6.4) \quad \max_{\mathbf{x} \in \Omega} \|B\boldsymbol{\tau}(\mathbf{x})\|_{\ell^\infty} \rightarrow 0 \quad \text{as } N \rightarrow \infty$$

if PHS are used. Note that, for fixed  $\mathbf{x} \in \Omega$ ,  $B\boldsymbol{\tau}(\mathbf{x})$  is an  $N$ -dimensional vector and  $\|B\boldsymbol{\tau}(\mathbf{x})\|_{\ell^\infty}$  denotes its  $\ell^\infty$ -norm. That is, the maximum absolute value of the  $N$  components. It should be pointed out that while (6.4) was numerically demonstrated only for PHS the relations (6.1) and (6.3) hold for general RBFs, assuming that  $\Phi$  and  $P$  have full rank. Please see [4, Section 4] for more details. We also remark that (6.4) implies the weaker statement

$$(6.5) \quad \|B\boldsymbol{\tau}(\cdot)\|_{\ell^1} \rightarrow 0 \quad \text{in } L^1(\Omega) \quad \text{as } N \rightarrow \infty.$$

Here,  $B\boldsymbol{\tau}(\cdot)$  denotes a vector-valued function,  $B\boldsymbol{\tau} : \Omega \rightarrow \mathbb{R}^N$ . That is, for a fixed argument  $\mathbf{x} \in \Omega$ ,  $B\boldsymbol{\tau}(\mathbf{x})$  is an  $N$ -dimensional vector in  $\mathbb{R}^N$  and  $\|B\boldsymbol{\tau}(\mathbf{x})\|_{\ell^1}$  denotes the usual  $\ell^1$ -norm of this vector. Thus, (6.5) means that the integral of the  $\ell^1$ -norm of the vector-valued function  $B\boldsymbol{\tau}(\cdot)$  converges to zero as  $N \rightarrow \infty$ . The above condition is not just weaker than (6.4) (see Remark 6.4), but also more convenient to investigate stability of CFs. Indeed, we have the following results.

**Lemma 6.1.** *Let  $\omega \in L^\infty(\Omega)$ . Assume  $\Phi$  and  $P$  in (2.5) have full rank and assume (6.5) to hold. Then the two following statements are equivalent:*

- (a)  $\|\hat{\mathbf{w}}\|_{\ell^1} \rightarrow \|I\|_\infty$  for  $N \rightarrow \infty$
- (b)  $\|\mathbf{w}\|_{\ell^1} \rightarrow \|I\|_\infty$  for  $N \rightarrow \infty$

*That is, either both the pure and polynomial augmented RBF-CF are asymptotically stable or none is.*

A short discussion on the term ‘‘asymptotically stable’’ is subsequently provided in Remark 6.2.

*Proof.* Assume  $\Phi$  and  $P$  in (2.5) have full rank and assume (6.5) to hold. Then (6.3) follows and therefore

$$(6.6) \quad \begin{aligned} \|\mathbf{w}\|_{\ell^1} &\leq \|\hat{\mathbf{w}}\|_{\ell^1} + \|BI[\boldsymbol{\tau}]\|_{\ell^1}, \\ \|\hat{\mathbf{w}}\|_{\ell^1} &\leq \|\mathbf{w}\|_{\ell^1} + \|BI[\boldsymbol{\tau}]\|_{\ell^1}. \end{aligned}$$



Next, note that  $BI[\boldsymbol{\tau}] = I[B\boldsymbol{\tau}]$  and thus

$$(6.7) \quad \|BI[\boldsymbol{\tau}]\|_{\ell^1} = \sum_{n=1}^N |I[(B\boldsymbol{\tau})_n]| \leq I \left[ \sum_{n=1}^N |(B\boldsymbol{\tau})_n| \right] = I [\|B\boldsymbol{\tau}\|_{\ell^1}].$$

Since  $\omega \in L^\infty(\Omega)$  it follows that

$$(6.8) \quad \|BI[\boldsymbol{\tau}]\|_{\ell^1} \leq \|\omega\|_{L^\infty(\Omega)} \int_{\Omega} \|B\boldsymbol{\tau}(\mathbf{x})\|_{\ell^1} d\mathbf{x}.$$

Thus, by assuming that (6.5) holds, we get  $\|BI[\boldsymbol{\tau}]\|_{\ell^1} \rightarrow 0$  for fixed  $d \in \mathbb{N}$  and  $N \rightarrow \infty$ . Finally, substituting this into (6.6) yields the assertion.  $\blacksquare$

Essentially, Lemma 6.1 states that—under the listed assumptions—it is sufficient to consider asymptotic stability of the pure RBF-CF. Once asymptotic (in)stability is established for the pure RBF-CF, by Lemma 6.1, it also carries over to all corresponding augmented RBF-CFs. Interestingly, this is following our findings for compactly supported RBFs reported in Theorem 5.1. There, conditional stability was ensured independently of the degree of the augmented polynomials.

*Remark 6.2 (Asymptotic Stability).* We call a sequence of CFs with weights  $\mathbf{w}_N \in \mathbb{R}^N$  for  $N \in \mathbb{N}$  asymptotically stable if  $\|\mathbf{w}_N\|_{\ell^1} \rightarrow \|I\|_\infty$  for  $N \rightarrow \infty$ . Recall that  $\|\mathbf{w}_N\|_{\ell^1} = \|C_N\|_\infty$  if the weights  $\mathbf{w}_N$  correspond to the  $N$ -point CF  $C_N$ . It is easy to note that this is a weaker property than every single CF being stable, i. e.,  $\|\mathbf{w}_N\|_{\ell^1} = \|I\|_\infty$  for all  $N \in \mathbb{N}$ . That said, consulting (3.2), asymptotic stability is sufficient for the CF to converge for all functions that can be approximated arbitrarily accurate by RBFs w. r. t. the  $L^\infty(\Omega)$ -norm. Of course, the propagation of input errors might be suboptimal for every single CF.

Lemma 6.1 essentially makes two assumptions. (1)  $A$  and  $P$  are full rank matrices on the data set of data points; and (2) the condition (6.4) holds. In the two following remarks, we comment on these assumptions.

*Remark 6.3 (On the First Assumption of Lemma 6.1).* Although it might seem restrictive to require  $A$  and  $P$  to have full rank, there are often even more restrictive constraints in practical problems. For instance, when solving partial differential equations, the data points are usually required to be smoothly scattered in such a way that the distance between data points is kept roughly constant. For such data points, it seems unlikely to find  $A$  and  $P$  (for  $N$  being sufficiently larger than  $d$ ) to be singular. See [4] for more details.

*Remark 6.4 (On the Second Assumption of Lemma 6.1).* The second assumption for Lemma 6.1 to hold is that (6.5) is satisfied. That is, the integral of  $\|B\boldsymbol{\tau}(\cdot)\|_{\ell^1} : \Omega \rightarrow \mathbb{R}_0^+$  converges to zero as  $N \rightarrow \infty$ . This is a weaker condition than the maximum value of  $\|B\boldsymbol{\tau}(\cdot)\|_{\ell^1}$  converging to zero, which was numerically observed to hold for PHS in [4]. The relation between these conditions can be observed by applying Hölder's inequality (see, for instance, [79, Chapter 3]). Let  $1 \leq p, q \leq \infty$  with  $1/p + 1/q = 1$  and assume that  $\omega \in L^q(\Omega)$ . Then we have

$$(6.9) \quad \int_{\Omega} \|B\boldsymbol{\tau}(\mathbf{x})\|_{\ell^1} \omega(\mathbf{x}) d\mathbf{x} \leq \left( \int_{\Omega} \|B\boldsymbol{\tau}(\mathbf{x})\|_{\ell^1}^p d\mathbf{x} \right)^{1/p} \left( \int_{\Omega} \omega(\mathbf{x})^q d\mathbf{x} \right)^{1/q}.$$

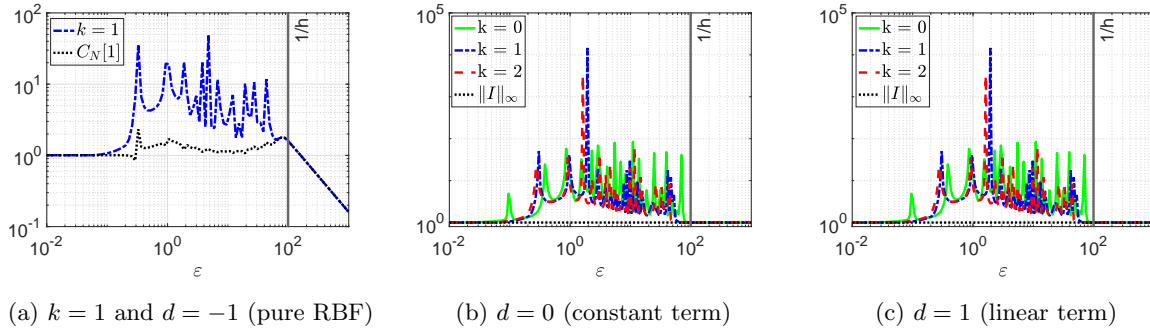


Figure 3: The stability measure  $\|C_N\|_\infty$  of Wendland’s compactly supported RBF  $\varphi_{1,k}$  with smoothness parameters  $k = 0, 1, 2$ . In all cases,  $N = 100$  equidistant data points were considered, while the reference shape parameter  $\varepsilon$  was allowed to vary.  $1/h$  denotes the threshold above which the basis functions have nonoverlapping support.

Hence,  $\|B\tau\|_{\ell^1}$  converging to zero in  $L^p(\Omega)$  as  $N \rightarrow \infty$  for some  $p \geq 1$  immediately implies (6.3). The special case of  $p = \infty$  corresponds to (6.4).

**7. Numerical Results.** We present a variety of numerical tests in one and two dimensions to demonstrate our theoretical findings. In particular, a stability and error analysis for CFs based on different RBFs is presented. Thereby, compactly supported RBFs are discussed in subsection 7.1, Gaussian RBFs in subsection 7.2, and PHS in subsection 7.3. For sake of simplicity, a constant weight function  $\omega \equiv 1$  is used in all test cases. All numerical tests presented here were generated by the open-access MATLAB code [41].

**7.1. Compactly Supported RBFs.** Let us start with a demonstration of Theorem 5.1 in one dimension. To this end, we consider Wendland’s compactly supported RBFs in  $\Omega = [0, 1]$ .

Figure 3 illustrates the stability measure  $\|C_N\|_\infty$  of Wendland’s compactly supported RBF  $\varphi_{1,k}$  with smoothness parameters  $k = 0, 1, 2$  as well as the optimal stability measure. The latter is given by  $C_N[1]$  if no constants are included and by  $\|I\|_\infty = 1$  if constants are included in the RBF approximations space, meaning that the RBF-CF is exact for constants. Furthermore,  $N = 100$  equidistant data points in  $\Omega = [0, 1]$  were used, including the end points,  $x_1 = 0$  and  $x_N = 1$ , and the (reference) shape parameter  $\varepsilon$  was allowed to vary. Finally,  $1/h$  denotes the threshold above which the compactly supported RBFs are all having nonoverlapping support.

We start by noting the RBF-CFs are observed to be stable for sufficiently small shape parameters. This can be explained by all the basis functions,  $\varphi_n$ , converging to a constant function for  $\varepsilon \rightarrow 0$ . At the same time, we can also observe the RBF-CF to be stable for  $\varepsilon \geq 1/h$ . It can be argued that this is in accordance with Theorem 5.1. Recall that Theorem 5.1 essentially states that for  $\varepsilon \geq 1/h$ , and assuming that all basis functions have equal moments ( $I[\varphi_n] = I[\varphi_m]$  for all  $n, m$ ), the corresponding RBF-CF (including polynomials of any degree) is stable if a sufficiently large number of equidistributed data points is used. Here, the equal moments condition was ensured by choosing the shape parameter as  $\varepsilon_n = \varepsilon$  for the interior

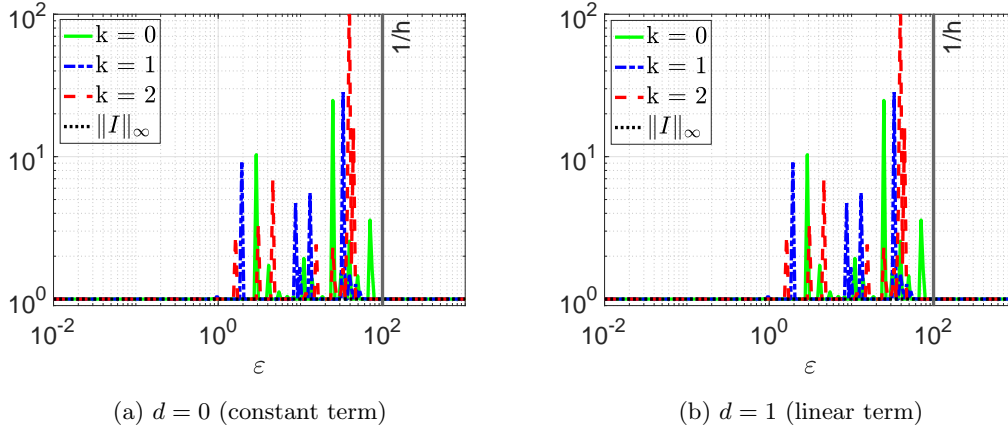


Figure 4: The stability measure  $\|C_N\|_\infty$  of Wendland's compactly supported RBF  $\varphi_{1,k}$  with smoothness parameters  $k = 0, 1, 2$ . In all cases,  $N = 100$  equidistant data points were considered. The same shape parameter  $\varepsilon$  was used for all basis functions, yielding (at least) the moments corresponding to the boundary data points  $x_1 = 0$  and  $x_N = 1$  to differ from the others.  $1/h$  denotes the threshold above which the basis functions have nonoverlapping support.

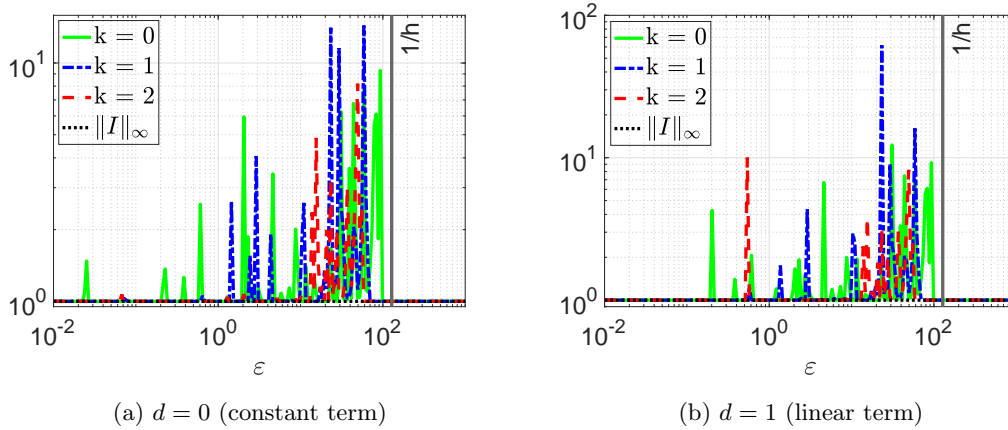


Figure 5: The stability measure  $\|C_N\|_\infty$  of Wendland's compactly supported RBF  $\varphi_{1,k}$  with smoothness parameters  $k = 0, 1, 2$ . In all cases,  $N = 100$  Halton points and a constant shape parameter  $\varepsilon$  were considered.  $1/h$  denotes the threshold above which the basis functions have nonoverlapping support.

data points ( $n = 2, \dots, N - 1$ ) and as  $\varepsilon_1 = \varepsilon_N = \varepsilon/2$  for the boundary data points.

That said, at least numerically, we observe that it is possible to drop this equal moment condition. This is demonstrated by [Figure 4](#), where we perform the same test as in [Figure 3](#) except choosing all the shape parameters to be equal ( $\varepsilon_n = \varepsilon$ ,  $n = 1, \dots, N$ ). This results in the two basis functions corresponding to the boundary points  $x_1 = 0$  and  $x_N = 1$  having

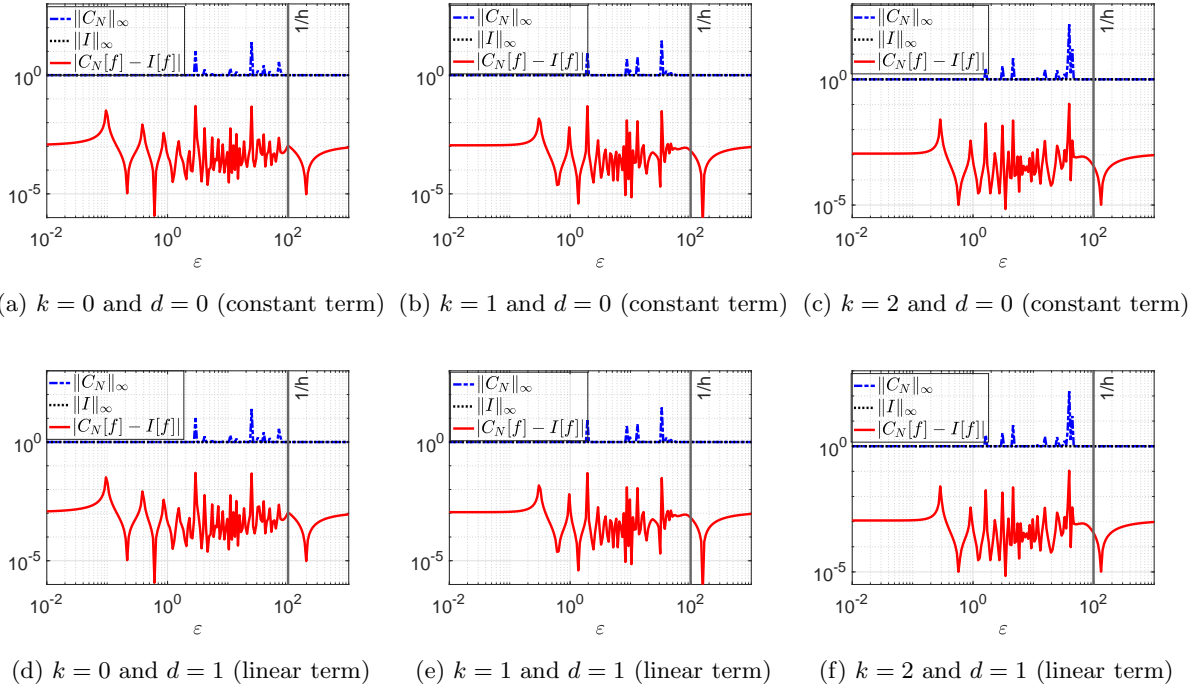


Figure 6: Error analysis for the one-dimensional test function  $f(x) = c/(1 + (x - 0.25)^2)$  on  $\Omega = [0, 1]$ , where  $c$  is chosen such that  $I[f] = 1$ . Illustrated are the error  $|I[f] - C_N[f]|$  and the stability measure  $\|C_N\|_\infty$  of Wendland's compactly supported RBF  $\varphi_{1,k}$  with smoothness parameters  $k = 0, 1, 2$ . In all cases,  $N = 100$  equidistant data points were considered, while the reference shape parameter  $\varepsilon$  was allowed to vary.  $1/h$  denotes the threshold above which the basis functions have nonoverlapping support.

smaller moments than the basis functions corresponding to interior data points for all  $\varepsilon$ . Nevertheless, we can see in [Figure 4](#) that for  $\varepsilon \geq 1/h$  the RBF-CFs are still stable. Moreover, the same observation is also made in [Figure 5](#) for the same test using Halton points. Once more, we find the corresponding RBF-CFs to be stable for  $\varepsilon \geq 1/h$  as well as for sufficiently small shape parameter  $\varepsilon$ .

To also provide an error analysis, [Figure 6](#) compares the stability measure  $\|C_N\|_\infty$  with the error of the RBF-CF for the Runge-like test function  $f(x) = c/(1 + (x - 0.25)^2)$  on  $\Omega = [0, 1]$ , where  $c$  is chosen such that  $I[f] = 1$ . Once more, we considered Wendland's compactly supported RBF  $\varphi_{1,k}$  with smoothness parameters  $k = 0, 1, 2$ ,  $N = 100$  equidistant data points, and a varying shape parameter  $\varepsilon$ , which is the same for all basis functions. There are a few observations that can be made based on the results reported in [Figure 6](#). Arguably most importantly, the smallest error seems to be obtained for a shape parameter that yields the RBF-CF to be stable ( $\|C_N\|_\infty = \|I\|_\infty$ ).

Next, we extend our numerical stability and error analysis to two dimensions, considering

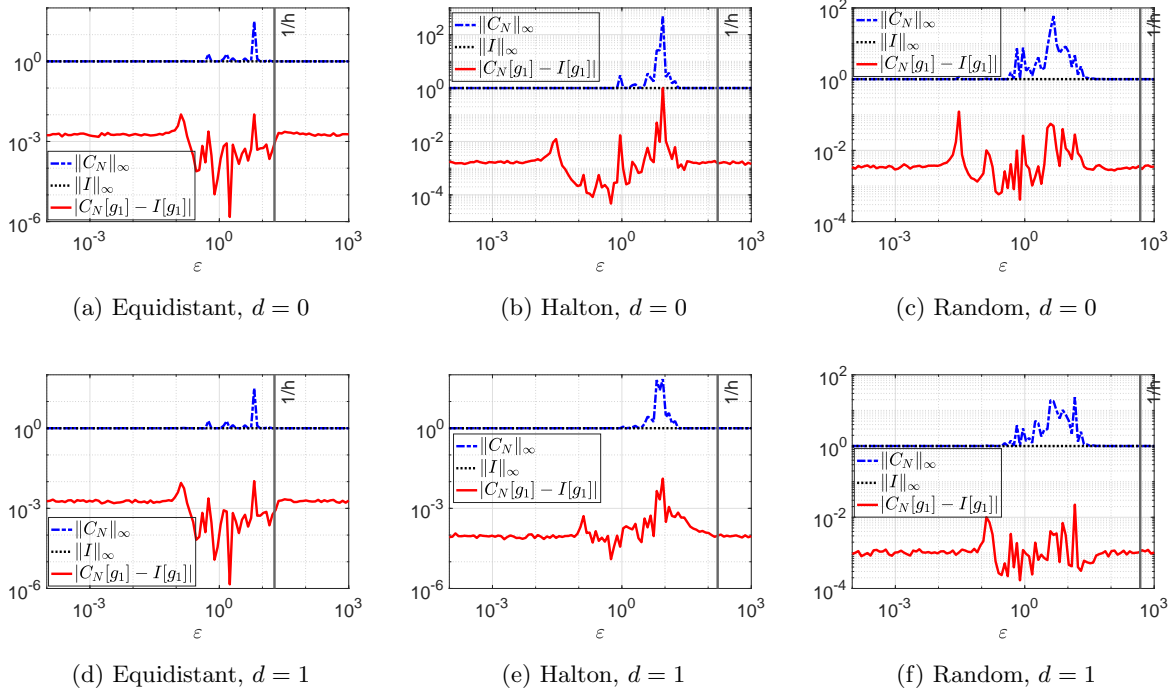


Figure 7: Error analysis for Wendland's compactly supported RBF  $\varphi_{2,k}$  in two dimensions with smoothness parameter  $k = 1$ . Considered is the first Genz test function  $g_1$  on  $\Omega = [0, 1]^2$ ; see (7.1). In all cases,  $N = 400$  data points (equidistant, Halton, or random) were considered, while the reference shape parameter  $\varepsilon$  was allowed to vary.  $1/h$  denotes the threshold above which the basis functions have nonoverlapping support.

the domain  $\Omega = [0, 1]^2$  and the following Genz test functions [35] (also see [90]):

$$\begin{aligned}
 (7.1) \quad g_1(\mathbf{x}) &= \cos\left(2\pi b_1 + \sum_{i=1}^q a_i x_i\right) && \text{(oscillatory),} \\
 g_2(\mathbf{x}) &= \prod_{i=1}^q \left(a_i^{-2} + (x_i - b_i)^2\right)^{-1} && \text{(product peak),} \\
 g_3(\mathbf{x}) &= \left(1 + \sum_{i=1}^q a_i x_i\right)^{-(q+1)} && \text{(corner peak),} \\
 g_4(\mathbf{x}) &= \exp\left(-\sum_{i=1}^q a_i^2 (x_i - b_i)^2\right) && \text{(Gaussian)}
 \end{aligned}$$

Here,  $q$  denotes the dimension under consideration and is henceforth chosen as  $q = 2$ . These functions are designed to have different difficult characteristics for numerical integration rou-

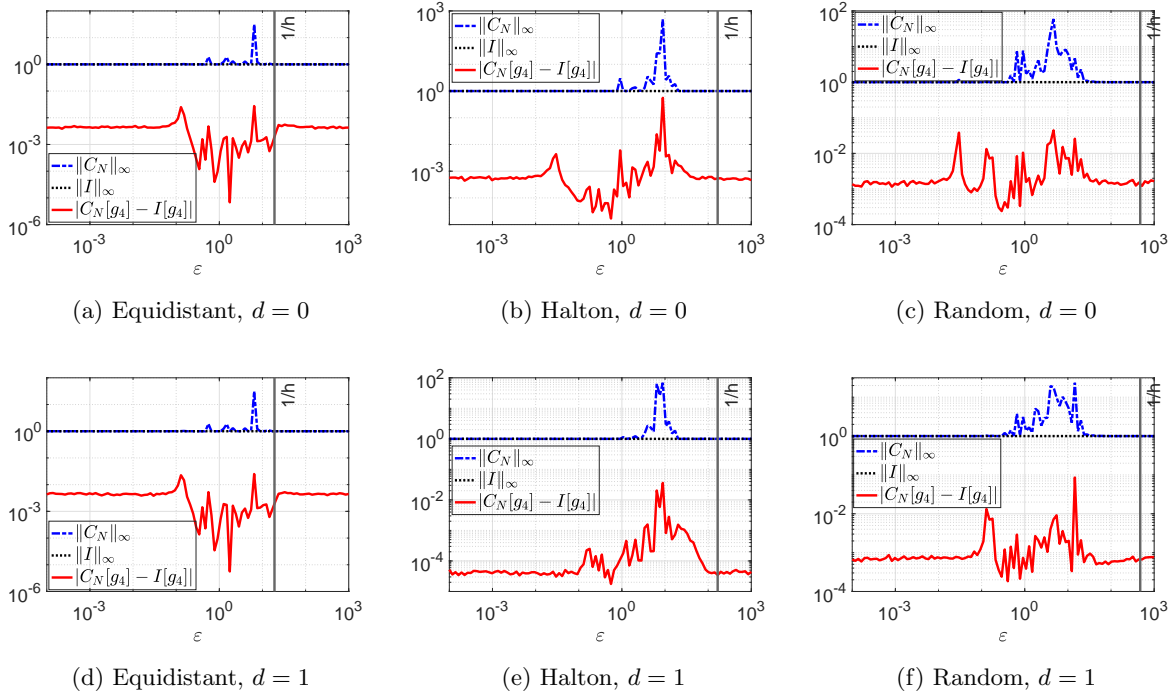


Figure 8: Error analysis for Wendland's compactly supported RBF  $\varphi_{2,k}$  in two dimensions with smoothness parameter  $k = 1$ . Considered is the fourth Genz test function  $g_4$  on  $\Omega = [0, 1]^2$ ; see (7.1). In all cases,  $N = 400$  data points (equidistant, Halton, or random) were considered, while the reference shape parameter  $\varepsilon$  was allowed to vary.  $1/h$  denotes the threshold above which the basis functions have nonoverlapping support.

times. The vectors  $\mathbf{a} = (a_1, \dots, a_q)^T$  and  $\mathbf{b} = (b_1, \dots, b_q)^T$  respectively contain (randomly chosen) shape and translation parameters. For each case, the experiment was repeated 100 times. At the same time, for each experiment, the vectors  $\mathbf{a}$  and  $\mathbf{b}$  were drawn randomly from  $[0, 1]^2$ . For reasons of space, we only report the results for  $g_1$  and  $g_4$  as well as  $k = 1$ . These can be found in Figure 7 and Figure 8, respectively. As before, the smallest errors are found for shape parameters that correspond to the RBF-CF being stable. The results for  $g_2, g_3$  and  $k = 0, 2$  are similar and can be found as part of the open-access MATLAB code [41].

It might be hard to identify the smallest errors as well as the corresponding shape parameter and stability measure from Figure 7 and Figure 8. Hence, these are listed separately in Table 2.

**7.2. Gaussian RBF.** Here, we perform a similar investigation of stability and accuracy as in subsection 7.1 for the Gaussian RBF, given by  $\varphi(r) = \exp(-\varepsilon^2 r^2)$ .

In particular, Figure 9 reports on the stability measure  $\|C_N\|_\infty$  for the Gaussian RBF-CF and the corresponding errors for the first and fourth Genz test function on  $\Omega = [0, 1]^2$  for  $N = 400$  data points. These are given as equidistant, Halton and random points, respectively. Furthermore, the shape parameter was allowed to vary from  $10^{-4}$  to  $10^3$  and the RBF-CF was

	$g_1$			$g_4$		
	$e_{\min}$	$\varepsilon$	$\ C_N\ _{\infty}$	$e_{\min}$	$\varepsilon$	$\ C_N\ _{\infty}$
Equidistant Points						
$d = 0$	1.4e-06	1.7e+00	1.0e+00	5.6e-06	1.7e+00	1.0e+00
$d = 1$	1.7e-06	1.7e+00	1.0e+00	6.2e-06	1.7e+00	1.0e+00
Halton Points						
$d = 0$	5.0e-05	5.5e-01	1.0e+00	2.0e-05	5.5e-01	1.0e+00
$d = 1$	1.1e-05	5.5e-01	1.0e+00	1.4e-05	5.5e-01	1.0e+00
Random Points						
$d = 0$	4.1e-04	7.7e-01	1.0e+00	1.6e-04	7.7e-01	1.0e+00
$d = 1$	2.3e-04	2.9e-01	1.0e+00	1.8e-04	4.0e-01	1.0e+00

Table 2: Minimal errors,  $e_{\min}$ , for the first and fourth Genz test function,  $g_1$  and  $g_4$ , together with the corresponding shape parameter,  $\varepsilon$ , and stability measure,  $\|C_N\|_{\infty}$ . In all cases, Wendland’s compactly supported RBF with smoothness parameter  $k = 1$  was used.

computed by augmenting the RBF basis with no ( $d = -1$ ) polynomials, a constant ( $d = 0$ ), or a linear term ( $d = 1$ ). Also for the Gaussian RBFs, we observe the RBF-CFs to be stable for a sufficiently large shape parameter. It might be argued that this is because the Gaussian RBF can be considered as being “close” to a compactly supported RBF for large shape parameter.<sup>4</sup> At the same time, however, the Gaussian RBF-CF are observed to become unstable for decreasing shape parameter  $\varepsilon$ . Furthermore, we observe the smallest error to occur in a region of instability in this case. Roughly speaking, this shape parameter—providing a minimal error—usually lies slightly below the smallest shape parameter that yields a stable RBF-CF. This might be explained by this shape parameter balancing out the two terms in (3.2). On the one hand, the RBF space  $\mathcal{S}_{N,d,\varepsilon}$  should provide a best approximation that is as close as possible to the underlying function,  $f$ . This is reflected in the term  $\|f - s\|_{L^\infty(\Omega)}$  on the right hand side of (3.2). On the other hand, the stability measure of the corresponding RBF-CF should be as small as possible. This is reflected in the term  $\|I\|_{\infty} + \|C_N\|_{\infty}$ , by which  $\|f - s\|_{L^\infty(\Omega)}$  is multiplied in (3.2). While for Gaussian RBFs the best approximation becomes more accurate for a decreasing shape parameter, the stability measure benefits from increasing shape parameters. In this case, the balance between these two objectives—and therefore the smallest error—is found outside of the region of stability.

That said, the situation changes if the data (function values) used in the RBF-CFs are perturbed by noise, which is often the case in applications. Such a situation is reported in

<sup>4</sup>Of course, strictly speaking, the Gaussian RBF does not have compact support. Yet, for large  $\varepsilon^2 r^2$  its function value will lie below machine precision, making it compactly supported in a numerical sense.



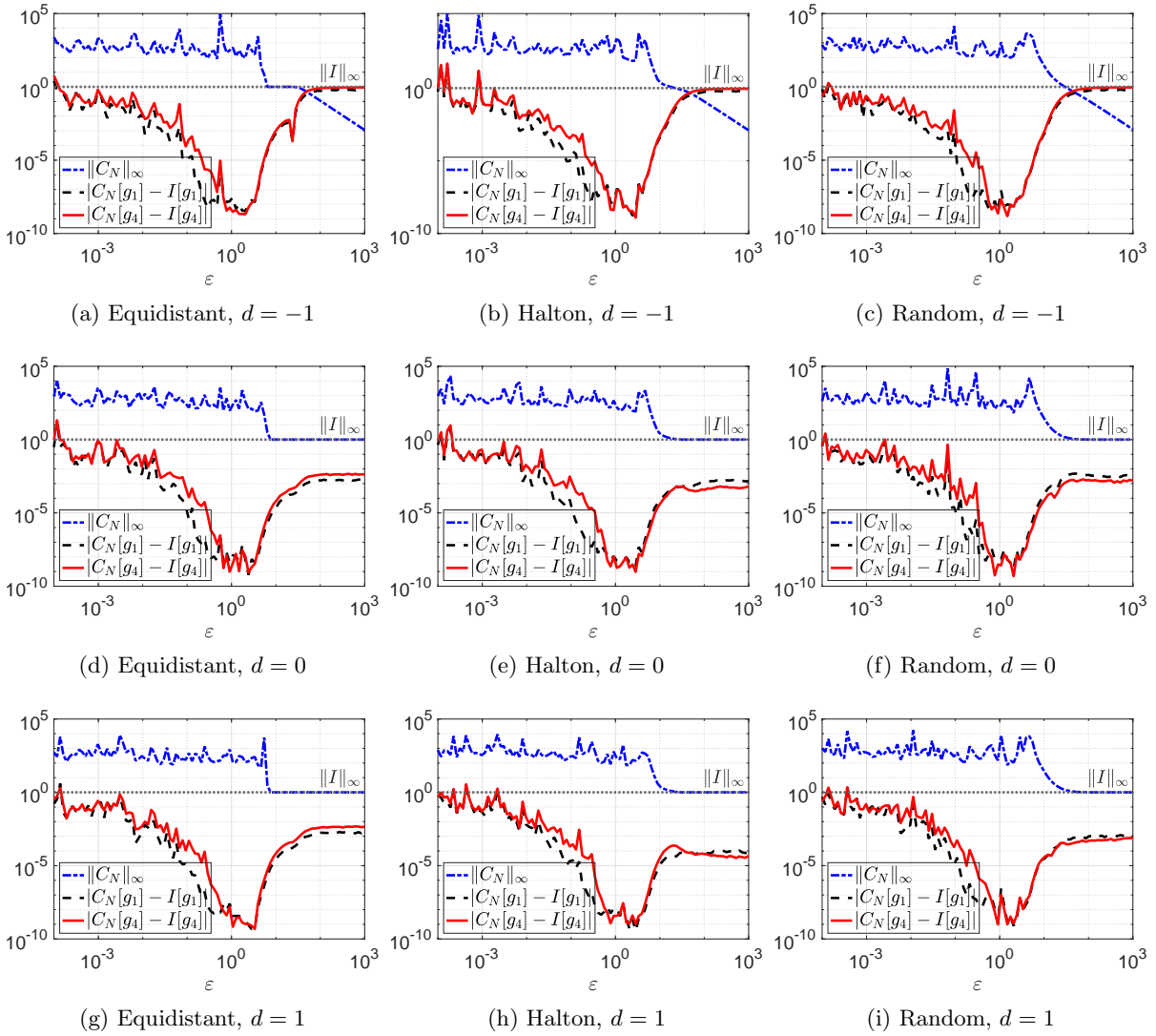


Figure 9: Error analysis for the Gaussian RBF  $\varphi(r) = \exp(\varepsilon^2 r^2)$  in two dimensions for the first and fourth Genz test function  $g_1, g_4$  on  $\Omega = [0, 1]^2$ ; see (7.1). In all cases,  $N = 400$  data points (equidistant, Halton, or random) were considered, while the reference shape parameter  $\varepsilon$  was allowed to vary.

**Figure 10.** Here, uniform white noise  $\mathbf{n} \in \mathbb{R}^N$  with  $\|\mathbf{n}\|_\infty \leq 10^{-4}$  was added to the function values of the first and fourth Genz test function. As a result, the term including the stability measure  $\|C_N\|_\infty$  in (3.2) gains in importance. In accordance with this, the minimal errors in Figure 10 are now attained for larger shape parameters that correspond to the RBF-CF having a smaller stability measure  $\|C_N\|_\infty$  as before. Also see Table 3 and Table 4 below. In particular, this demonstrates the increased importance of stability of CF when these are used in real-world applications where the presence of noise can often not be avoided.

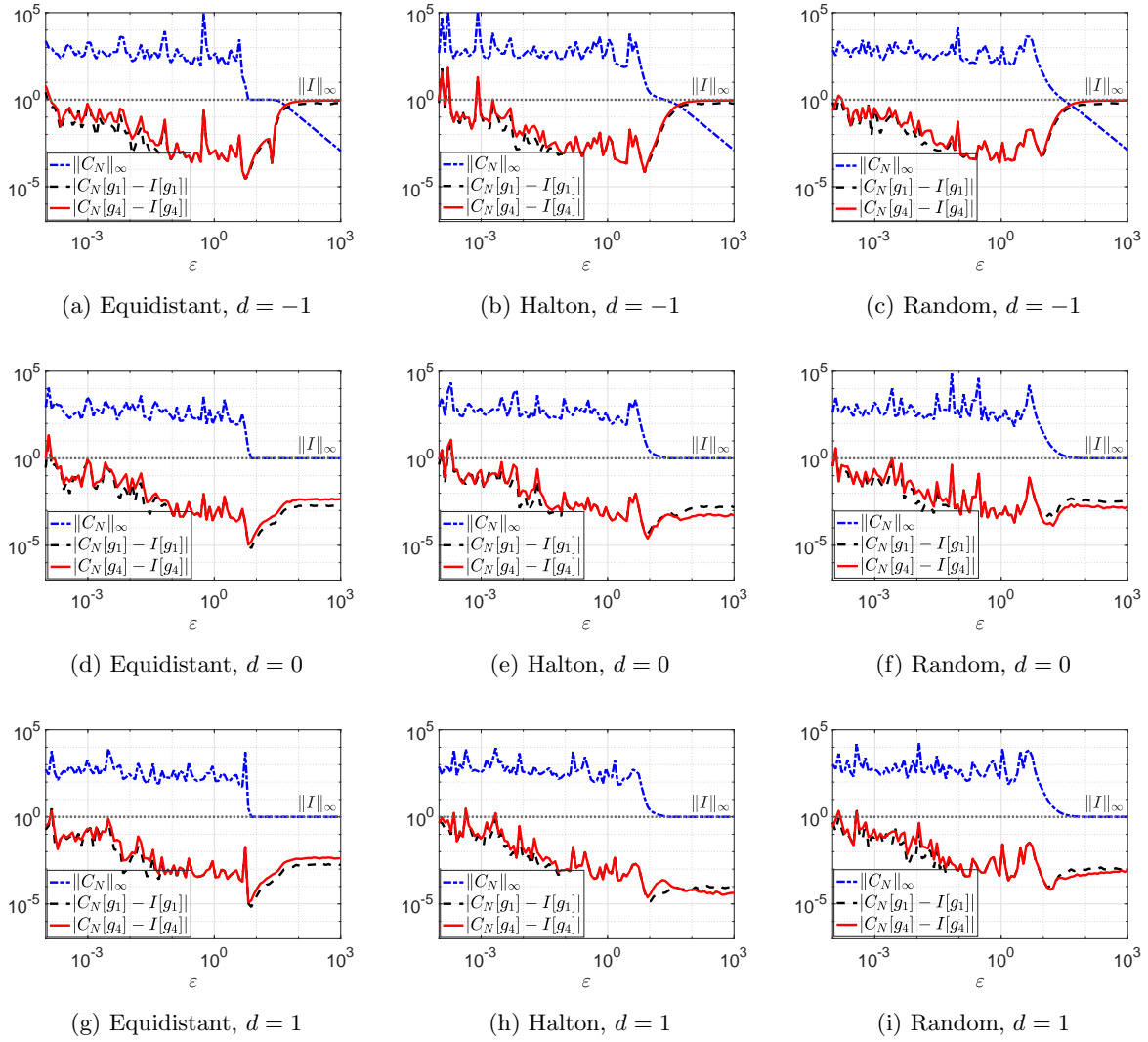


Figure 10: Error analysis for the Gaussian RBF  $\varphi(r) = \exp(\varepsilon^2 r^2)$  in two dimensions for the first and fourth Genz test function  $g_1, g_4$  on  $\Omega = [0, 1]^2$ ; see (7.1). Uniform white noise  $\mathbf{n} \in \mathbb{R}^N$  with  $\|\mathbf{n}\|_\infty \leq 10^{-4}$  was added to the function values. In all cases,  $N = 400$  data points (equidistant, Halton, or random) were considered, while the reference shape parameter  $\varepsilon$  was allowed to vary.

It might be hard to identify the smallest errors as well as the corresponding shape parameter and stability measure from Figure 9 and Figure 10. Hence, these are listed separately in Table 3 and Table 4 for the first and fourth Genz test function with and without noise, respectively.

**7.3. Polyharmonic Splines.** We end this section by providing a similar investigation for PHS. Again, the first and fourth Genz test functions on  $\Omega = [0, 1]^2$  are considered. However,

	$g_1$ without noise			$g_1$ with noise		
	$e_{\min}$	$\varepsilon$	$\ C_N\ _{\infty}$	$e_{\min}$	$\varepsilon$	$\ C_N\ _{\infty}$
Equidistant Points						
$d = 0$	6.1e-10	2.4e+00	1.1e+02	6.6e-06	7.5e+00	1.0e+00
$d = 1$	5.4e-10	3.3e+00	2.6e+02	6.7e-06	7.5e+00	1.0e+00
Halton Points						
$d = 0$	2.4e-09	2.8e+00	8.1e+01	4.6e-05	8.9e+00	3.9e+00
$d = 1$	4.1e-10	2.8e+00	1.4e+02	1.3e-05	1.0e+01	2.2e+00
Random Points						
$d = 0$	1.5e-09	2.0e+00	6.4e+01	1.9e-04	2.0e+00	6.4e+01
$d = 1$	7.8e-10	2.0e+00	1.0e+02	9.1e-05	1.2e+01	1.0e+01

Table 3: Minimal errors,  $e_{\min}$ , for the first Genz test function,  $g_1$ , with and without noise together with the corresponding shape parameter,  $\varepsilon$ , and stability measure,  $\|C_N\|_{\infty}$ . In all cases, the Gaussian RBF was used.

for PHS no shape parameter is involved and we therefore consider their stability and accuracy for an increasing number of equidistant, Halton and random data points. The results for the TPS ( $\varphi(r) = r^2 \log r$ ), cubic ( $\varphi(r) = r^3$ ) and quintic ( $\varphi(r) = r^5$ ) PHS RBFs can be found in [Figure 11](#). In all cases, the corresponding PHS basis was augmented with a linear term ( $d = 1$ ). We can observe from [Figure 11](#) that all RBF-CFs converge (with the rate of convergence depending on the order of the PHS) while also remaining stable or at least being asymptotically stable. It would be of interest to provide a theoretical investigation on (asymptotic) stability of PHS-CFs and under which conditions this might be ensured. This might be addressed in future works.

**8. Concluding Thoughts.** In this work, we investigated stability of RBF-CFs. We started by showing that stability of RBF-CFs can be connected to the famous Lebesgue constant of the underlying RBF interpolant. While this indicates that RBF-CFs might benefit from low Lebesgue constants, it was also demonstrated that RBF-CFs often have superior stability properties compared to RBF interpolation. Furthermore, stability was proven for RBF-CFs based on compactly supported RBFs under the assumption of a sufficiently large number of (equidistributed) data points and the shape parameter(s) lying above a certain threshold. Finally, we showed that under certain conditions asymptotic stability of RBF-CFs is independent of polynomial terms that are usually included in RBF approximations. The above findings were accompanied by a series of numerical tests.

While we believe this work to be a valuable step towards a more mature stability theory of RBF-CFs, the present work also demonstrates that further steps in this direction would be

	$g_4$ without noise			$g_4$ with noise		
	$e_{\min}$	$\varepsilon$	$\ C_N\ _{\infty}$	$e_{\min}$	$\varepsilon$	$\ C_N\ _{\infty}$
Equidistant Points						
$d = 0$	7.8e-10	2.4e+00	1.1e+02	1.0e-05	6.4e+00	3.1e+00
$d = 1$	4.6e-10	3.3e+00	2.6e+02	1.0e-05	6.4e+00	3.1e+00
Halton Points						
$d = 0$	1.0e-09	2.8e+00	8.1e+01	2.8e-05	8.9e+00	3.9e+00
$d = 1$	1.0e-09	2.8e+00	1.4e+02	2.0e-05	8.9e+00	3.9e+00
Random Points						
$d = 0$	4.8e-10	2.0e+00	6.4e+01	1.3e-04	1.7e+01	3.6e+00
$d = 1$	9.7e-10	9.1e-01	1.5e+02	6.6e-05	1.4e+01	5.7e+00

Table 4: Minimal errors,  $e_{\min}$ , for the fourth Genz test function,  $g_4$ , with and without noise together with the corresponding shape parameter,  $\varepsilon$ , and stability measure,  $\|C_N\|_{\infty}$ . In all cases, the Gaussian RBF was used.

highly welcome.

### Appendix A. Moments.

Henceforth, we provide the moments for different RBFs. The one-dimensional case is discussed in [Appendix A.1](#), while two-dimensional moments are derived in [Appendix A.2](#).

**A.1. One-Dimensional Moments.** Let us consider the one-dimensional case of  $\Omega = [a, b]$  and distinct data points  $x_1, \dots, x_N \in [a, b]$ .

**A.1.1. Gaussian RBF.** For  $\varphi(r) = \exp(-\varepsilon^2 r^2)$ , the moment of the translated Gaussian RBF,

$$(A.1) \quad m_n = m(\varepsilon, x_n, a, b) = \int_a^b \exp(-\varepsilon^2 |x - x_n|^2) dx,$$

is given by

$$(A.2) \quad m_n = \frac{\sqrt{\pi}}{2\varepsilon} [\operatorname{erf}(\varepsilon(b - x_n)) - \operatorname{erf}(\varepsilon(a - x_n))].$$

Here,  $\operatorname{erf}(x) = 2/\sqrt{\pi} \int_0^x \exp(-t^2) dt$  denotes the usual *error function*, [[72](#), Section 7.2].

**A.1.2. Polyharmonic Splines.** For  $\varphi(r) = r^k$  with odd  $k \in \mathbb{N}$ , the moment of the translated PHS,

$$(A.3) \quad m_n = m(x_n, a, b) = \int_a^b \varphi(x - x_n) dx,$$

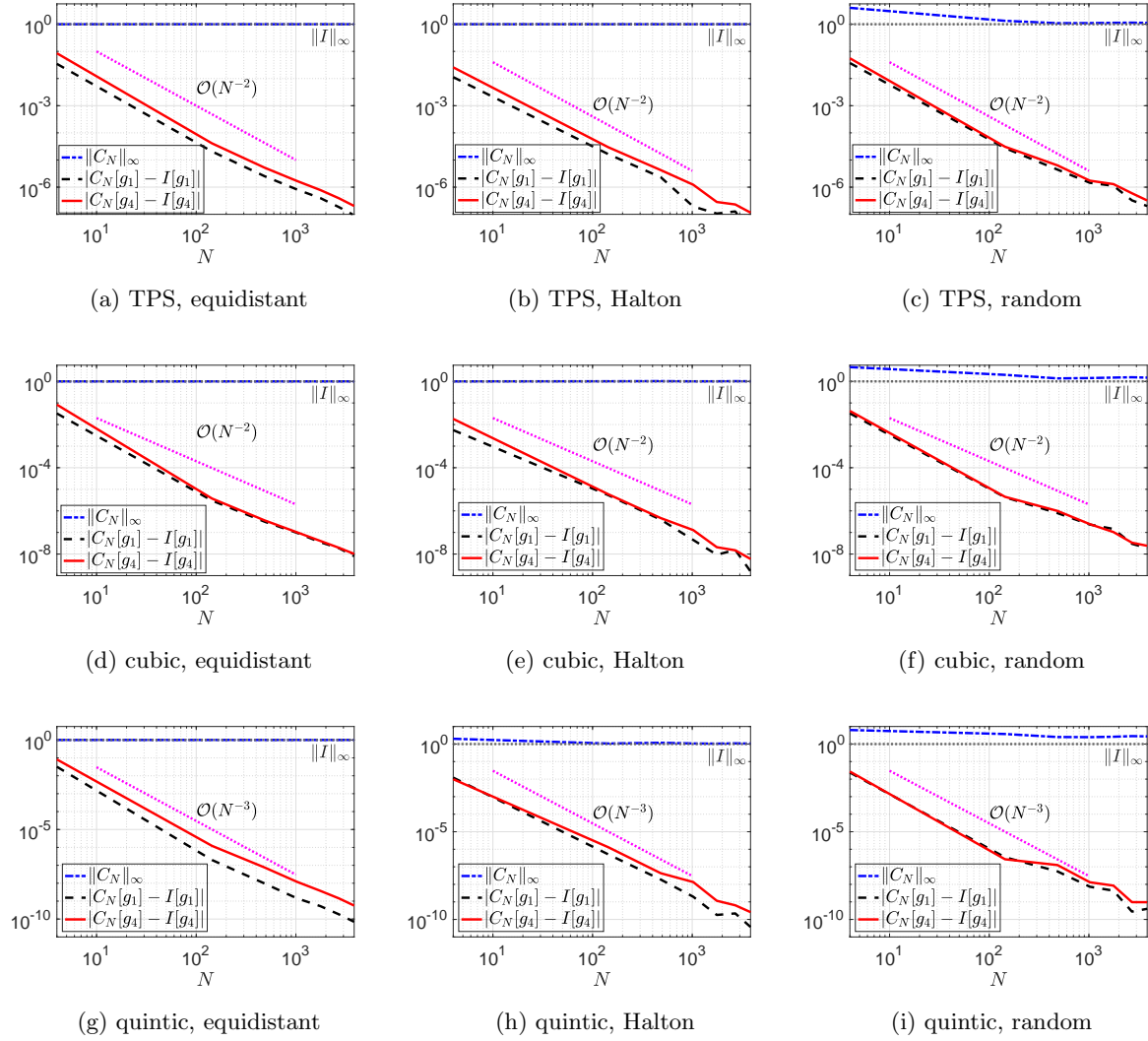


Figure 11: Error analysis for the TPS ( $\varphi(r) = r^2 \log r$ ), cubic ( $\varphi(r) = r^3$ ) and quintic ( $\varphi(r) = r^5$ ) in two dimensions. The first and fourth Genz test functions  $g_1, g_4$  were considered on  $\Omega = [0, 1]^2$ ; see (7.1). In all cases, linear terms were incorporated, i. e.,  $d = 1$ .

is given by

$$(A.4) \quad m_n = \frac{1}{k+1} \left[ (a-x_n)^{k+1} + (b-x_n)^{k+1} \right], \quad n = 1, 2, \dots, N.$$

For  $\varphi(r) = r^k \log r$  with even  $k \in \mathbb{N}$ , on the other hand, we have

$$(A.5) \quad m_n = (x_n - a)^{k+1} \left[ \frac{\log(x_n - a)}{k+1} - \frac{1}{(k+1)^2} \right] + (b - x_n)^{k+1} \left[ \frac{\log(b - x_n)}{k+1} - \frac{1}{(k+1)^2} \right].$$

Note that for  $x_n = a$  the first term is zero, while for  $x_n = b$  the second term is zero.

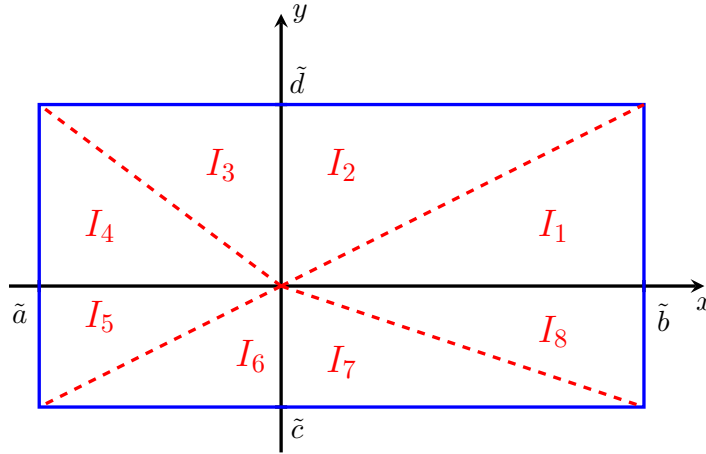


Figure 12: Illustration of how the moments can be computed on a rectangle in two dimensions

**A.2. Two-Dimensional Moments.** Here, we consider the two-dimensional case, where the domain is given by a rectangular of the form  $\Omega = [a, b] \times [c, d]$ .

**A.2.1. Gaussian RBF.** For  $\varphi(r) = \exp(-\varepsilon^2 r^2)$ , the two-dimensional moments can be written as products of one-dimensional moments. In fact, we have

$$(A.6) \quad \int_a^b \int_c^d \exp(-\varepsilon^2 \|(x - x_n, y - y_n)\|_2^2) = m(\varepsilon, x_n, a, b) \cdot m(\varepsilon, y_n, c, d).$$

Here, the multiplicands on the right-hand side are the one-dimensional moments from (A.1).

**A.2.2. Polyharmonic Splines and Other RBFs.** If it is not possible to trace the two-dimensional moments back to the one-dimensional ones, we are in need of another approach. This is, for instance, the case for PHS. We start by noting that for a data points  $(x_n, y_n) \in [a, b] \times [c, d]$  the corresponding moment can be rewritten as follows:

$$(A.7) \quad m(x_n, y_n) = \int_a^b \int_c^d \varphi(\|(x - x_n, y - y_n)^T\|_2) \, dy \, dx = \int_{\tilde{a}}^{\tilde{b}} \int_{\tilde{c}}^{\tilde{d}} \varphi(\|(x, y)^T\|_2) \, dy \, dx$$

with translated boundaries  $\tilde{a} = a - x_n$ ,  $\tilde{b} = b - x_n$ ,  $\tilde{c} = c - y_n$ , and  $\tilde{d} = d - y_n$ . We are not aware of an explicit formula for such integrals for most popular RBFs readily available from the literature. That said, such formulas were derived in [76, 78, 77] (also see [91, Chapter 2.3]) for the integral of  $\varphi$  over a *right triangle* with vertices  $(0, 0)^T$ ,  $(\alpha, 0)^T$ , and  $(\alpha, \beta)^T$ . Assuming  $\tilde{a} < 0 < \tilde{b}$  and  $\tilde{c} < 0 < \tilde{d}$ , we therefore partition the shifted domain  $\tilde{\Omega} = [\tilde{a}, \tilde{b}] \times [\tilde{c}, \tilde{d}]$  into eight right triangles. Denoting the corresponding integrals by  $I_1, \dots, I_8$ , the moment  $m(x_n, y_n)$  correspond to the sum of these integrals. The procedure is illustrated in Figure 12.

The special cases where one (or two) of the edges of the rectangle align with one of the axes can be treated similarly. However, in this case, a smaller subset of the triangles is considered.

$\varphi(r)$	$I_{\text{ref}}(\alpha, \beta)$
$r^2 \log r$	$\frac{\alpha}{144} \left[ 24\alpha^3 \arctan(\beta/\alpha) + 6\beta(3\alpha^2 + \beta^2) \log(\alpha^2 + \beta^2) - 33\alpha^2\beta - 7\beta^3 \right]$
$r^3$	$\frac{\alpha}{40} \left[ 3\alpha^4 \operatorname{arcsinh}(\beta/\alpha) + \beta(5\alpha^2 + 2\beta^2) \sqrt{\alpha^2 + \beta^2} \right]$
$r^5$	$\frac{\alpha}{336} \left[ 15\alpha^6 \operatorname{arcsinh}(\beta/\alpha) + \beta(33\alpha^4 + 26\alpha^2\beta^2 + 8\beta^4) \sqrt{\alpha^2 + \beta^2} \right]$
$r^7$	$\frac{\alpha}{3346} \left[ 105\alpha^8 \operatorname{arcsinh}(\beta/\alpha) + \beta(279\alpha^6 + 326\alpha^4\beta^2 + 200\alpha^2\beta^4 + 48\beta^6) \sqrt{\alpha^2 + \beta^2} \right]$

Table 5: The reference integral  $I_{\text{ref}}(\alpha, \beta)$ —see (A.9)—for some PHS

We leave the details to the reader, and note the following formula for the weights:

$$(A.8) \quad m(x_n, y_n) = \left[ 1 - \delta_0(\tilde{b}\tilde{d}) \right] (I_1 + I_2) + \left[ 1 - \delta_0(\tilde{a}\tilde{d}) \right] (I_3 + I_4) \\ + \left[ 1 - \delta_0(\tilde{a}\tilde{c}) \right] (I_5 + I_6) + \left[ 1 - \delta_0(\tilde{b}\tilde{c}) \right] (I_7 + I_8)$$

Here,  $\delta_0$  denotes the usual Kronecker delta defined as  $\delta_0(x) = 1$  if  $x = 0$  and  $\delta_0(x) = 0$  if  $x \neq 0$ . The above formula holds for general  $\tilde{a}$ ,  $\tilde{b}$ ,  $\tilde{c}$ , and  $\tilde{d}$ . Note that all the right triangles can be rotated or mirrored in a way that yields a corresponding integral of the form

$$(A.9) \quad I_{\text{ref}}(\alpha, \beta) = \int_0^\alpha \int_0^{\frac{\beta}{\alpha}x} \varphi(\|(x, y)^T\|_2) dy dx.$$

More precisely, we have

$$(A.10) \quad I_1 = I_{\text{ref}}(\tilde{b}, \tilde{d}), \quad I_2 = I_{\text{ref}}(\tilde{d}, \tilde{b}), \quad I_3 = I_{\text{ref}}(\tilde{d}, -\tilde{a}), \quad I_4 = I_{\text{ref}}(-\tilde{a}, \tilde{d}), \\ I_5 = I_{\text{ref}}(-\tilde{a}, -\tilde{c}), \quad I_6 = I_{\text{ref}}(-\tilde{c}, -\tilde{a}), \quad I_7 = I_{\text{ref}}(-\tilde{c}, \tilde{b}), \quad I_8 = I_{\text{ref}}(\tilde{b}, -\tilde{c}).$$

Finally, explicit formulas of the reference integral  $I_{\text{ref}}(\alpha, \beta)$  over the right triangle with vertices  $(0, 0)^T$ ,  $(\alpha, 0)^T$ , and  $(\alpha, \beta)^T$  for some PHS can be found in Table 5. Similar formulas are also available, for instance, for Gaussian, multiquadric and inverse multiquadric RBFs.

We note that the approach presented above is similar to the one in [84], where the domain  $\Omega = [-1, 1]^2$  was considered. Later, the same authors extended their findings to simple polygons [83] using the Gauss–Green theorem. Also see the recent work [85], addressing polygonal regions that may be nonconvex or even multiply connected, and references therein. It would be of interest to see if these approaches also carry over to computing products of RBFs corresponding to different centers or products of RBFs and their partial derivatives, again corresponding to different centers. Such integrals occur as elements of mass and stiffness matrices in numerical PDEs. In particular, they are desired to construct linearly energy stable (global) RBF methods for hyperbolic conservation laws [37, 42, 43].

## REFERENCES



- [1] W. F. AMES, *Numerical Methods for Partial Differential Equations*, Academic press, 2014.
- [2] I. AZIZ, W. KHAN, ET AL., *Numerical integration of multi-dimensional highly oscillatory, gentle oscillatory and non-oscillatory integrands based on wavelets and radial basis functions*, *Engineering Analysis with Boundary Elements*, 36 (2012), pp. 1284–1295.
- [3] V. BAYONA, *Comparison of moving least squares and RBF+poly for interpolation and derivative approximation*, *Journal of Scientific Computing*, 81 (2019), pp. 486–512.
- [4] V. BAYONA, *An insight into RBF-FD approximations augmented with polynomials*, *Computers & Mathematics with Applications*, 77 (2019), pp. 2337–2353.
- [5] L. BOS, M. CALIARI, S. DE MARCHI, M. VIANELLO, AND Y. XU, *Bivariate Lagrange interpolation at the Padua points: the generating curve approach*, *Journal of Approximation Theory*, 143 (2006), pp. 15–25.
- [6] L. BOS AND S. DE MARCHI, *Univariate radial basis functions with compact support cardinal functions*, *East Journal on Approximations*, 14 (2008), p. 69.
- [7] L. BOS, S. DE MARCHI, M. VIANELLO, AND Y. XU, *Bivariate Lagrange interpolation at the Padua points: the ideal theory approach*, *Numerische Mathematik*, 108 (2007), pp. 43–57.
- [8] H. BRASS, *Quadraturverfahren*, vol. 3, Vandenhoeck+ Ruprecht Gm, 1977.
- [9] H. BRASS AND K. PETRAS, *Quadrature Theory: The Theory of Numerical Integration on a Compact Interval*, no. 178 in *Mathematical Surveys and Monographs*, American Mathematical Society, 2011.
- [10] L. BRUTMAN, *Lebesgue functions for polynomial interpolation—a survey*, *Annals of Numerical Mathematics*, 4 (1996), pp. 111–128.
- [11] M. D. BUHMANN, *Radial basis functions*, *Acta Numerica*, 9 (2000), pp. 1–38.
- [12] M. D. BUHMANN, *Radial Basis Functions: Theory and Implementations*, vol. 12, Cambridge University Press, 2003.
- [13] R. E. CAFLISCH, *Monte Carlo and quasi-Monte Carlo methods*, *Acta Numerica*, 1998 (1998), pp. 1–49.
- [14] R. COOLS, *Constructing cubature formulae: The science behind the art*, *Acta Numerica*, 6 (1997), pp. 1–54.
- [15] R. COOLS, *An encyclopaedia of cubature formulas*, *Journal of Complexity*, 19 (2003), pp. 445–453.
- [16] R. COOLS, I. MYSOVSKIKH, AND H. SCHMID, *Cubature formulae and orthogonal polynomials*, *Journal of Computational and Applied Mathematics*, 127 (2001), pp. 121–152.
- [17] P. J. DAVIS AND P. RABINOWITZ, *Methods of Numerical Integration*, Courier Corporation, 2007.
- [18] S. DE MARCHI, *On optimal center locations for radial basis function interpolation: computational aspects*, *Rend. Splines Radial Basis Functions and Applications*, 61 (2003), pp. 343–358.
- [19] S. DE MARCHI AND G. SANTIN, *A new stable basis for radial basis function interpolation*, *Journal of Computational and Applied Mathematics*, 253 (2013), pp. 1–13.
- [20] S. DE MARCHI AND R. SCHABACK, *Stability of kernel-based interpolation*, *Advances in Computational Mathematics*, 32 (2010), pp. 155–161.
- [21] J. DICK, F. Y. KUO, AND I. H. SLOAN, *High-dimensional integration: The quasi-Monte Carlo way*, *Acta Numerica*, 22 (2013), p. 133.
- [22] T. A. DRISCOLL AND B. FORNBERG, *Interpolation in the limit of increasingly flat radial basis functions*, *Computers & Mathematics with Applications*, 43 (2002), pp. 413–422.
- [23] H. ENGELS, *Numerical Quadrature and Cubature*, Academic Press, 1980.
- [24] G. E. FASSHAUER, *Solving partial differential equations by collocation with radial basis functions*, in *Proceedings of Chamonix*, vol. 1997, Vanderbilt University Press Nashville, TN, 1996, pp. 1–8.
- [25] G. E. FASSHAUER, *Meshfree Approximation Methods with MATLAB*, vol. 6, World Scientific, 2007.
- [26] G. E. FASSHAUER AND M. J. MCCOURT, *Stable evaluation of Gaussian radial basis function interpolants*, *SIAM Journal on Scientific Computing*, 34 (2012), pp. A737–A762.
- [27] N. FLYER, G. A. BARNETT, AND L. J. WICKER, *Enhancing finite differences with radial basis functions: experiments on the Navier–Stokes equations*, *Journal of Computational Physics*, 316 (2016), pp. 39–62.
- [28] G. B. FOLLAND, *How to integrate a polynomial over a sphere*, *The American Mathematical Monthly*, 108 (2001), pp. 446–448.
- [29] B. FORNBERG AND N. FLYER, *A Primer on Radial Basis Functions With Applications to the Geosciences*, SIAM, 2015.
- [30] B. FORNBERG AND N. FLYER, *Solving PDEs with radial basis functions*, *Acta Numerica*, 24 (2015), pp. 215–258.

- [31] B. FORNBERG, E. LARSSON, AND N. FLYER, *Stable computations with Gaussian radial basis functions*, SIAM Journal on Scientific Computing, 33 (2011), pp. 869–892.
- [32] B. FORNBERG, E. LEHTO, AND C. POWELL, *Stable calculation of Gaussian-based RBF-FD stencils*, Computers & Mathematics with Applications, 65 (2013), pp. 627–637.
- [33] B. FORNBERG, G. WRIGHT, AND E. LARSSON, *Some observations regarding interpolants in the limit of flat radial basis functions*, Computers & Mathematics with Applications, 47 (2004), pp. 37–55.
- [34] E. FUSELIER, T. HANGELBROEK, F. J. NARCOWICH, J. D. WARD, AND G. B. WRIGHT, *Kernel based quadrature on spheres and other homogeneous spaces*, Numerische Mathematik, 127 (2014), pp. 57–92.
- [35] A. GENZ, *Testing multidimensional integration routines*, in Proc. of International Conference on Tools, Methods and Languages for Scientific and Engineering Computation, 1984, pp. 81–94.
- [36] P. GLASSERMAN, *Monte Carlo Methods in Financial Engineering*, vol. 53, Springer Science & Business Media, 2013.
- [37] J. GLAUBITZ, *Shock capturing and high-order methods for hyperbolic conservation laws*, Logos Verlag Berlin GmbH, 2020.
- [38] J. GLAUBITZ, *Stable high-order cubature formulas for experimental data*, arXiv:2009.11981, (2020). Submitted.
- [39] J. GLAUBITZ, *Stable high order quadrature rules for scattered data and general weight functions*, SIAM Journal on Numerical Analysis, 58 (2020), pp. 2144–2164.
- [40] J. GLAUBITZ, *Construction and application of provable positive and exact cubature formulas*, arXiv preprint arXiv:2108.02848, (2021).
- [41] J. GLAUBITZ, *jglaubit/stability-RBF-CFs*, 2021, <https://doi.org/10.5281/zenodo.5086347>. MATLAB code.
- [42] J. GLAUBITZ AND A. GELB, *Stabilizing radial basis function methods for conservation laws using weakly enforced boundary conditions*, Journal of Scientific Computing, 87 (2021), pp. 1–29.
- [43] J. GLAUBITZ, E. LE MELEDO, AND P. ÖFFNER, *Towards stable radial basis function methods for linear advection problems*, Computers & Mathematics with Applications, 85 (2021), pp. 84–97.
- [44] S. HABER, *Numerical evaluation of multiple integrals*, SIAM Review, 12 (1970), pp. 481–526.
- [45] J. H. HALTON, *On the efficiency of certain quasi-random sequences of points in evaluating multidimensional integrals*, Numerische Mathematik, 2 (1960), pp. 84–90.
- [46] R. L. HARDY, *Multiquadric equations of topography and other irregular surfaces*, Journal of Geophysical Research, 76 (1971), pp. 1905–1915.
- [47] J. S. HESTHAVEN AND T. WARBURTON, *Nodal Discontinuous Galerkin Methods: Algorithms, Analysis, and Applications*, Springer Science & Business Media, 2007.
- [48] E. HLAWKA, *Funktionen von beschränkter Variation in der Theorie der Gleichverteilung*, Ann. Mat. Pura Appl., 54 (1961), pp. 325–333.
- [49] D. HUYBRECHS, *Stable high-order quadrature rules with equidistant points*, Journal of Computational and Applied Mathematics, 231 (2009), pp. 933–947.
- [50] B. A. IBRAHIMOGLU, *Lebesgue functions and Lebesgue constants in polynomial interpolation*, Journal of Inequalities and Applications, 2016 (2016), pp. 1–15.
- [51] A. ISKE, *On the approximation order and numerical stability of local Lagrange interpolation by polyharmonic splines*, in Modern Developments in Multivariate Approximation, Springer, 2003, pp. 153–165.
- [52] A. ISKE, *Radial basis functions: basics, advanced topics and meshfree methods for transport problems*, Rend. Sem. Mat. Univ. Pol. Torino, 61 (2003), pp. 247–285.
- [53] A. ISKE, *Scattered data approximation by positive definite kernel functions*, Rend. Sem. Mat. Univ. Pol. Torino, 69 (2011), pp. 217–246.
- [54] A. ISKE AND T. SONAR, *On the structure of function spaces in optimal recovery of point functionals for ENO-schemes by radial basis functions*, Numerische Mathematik, 74 (1996), pp. 177–201.
- [55] E. KANSA AND Y. HON, *Circumventing the ill-conditioning problem with multiquadric radial basis functions: Applications to elliptic partial differential equations*, Computers and Mathematics with Applications, 39 (2000), pp. 123–138.
- [56] E. J. KANSA, *Multiquadrics—a scattered data approximation scheme with applications to computational fluid-dynamics—ii Solutions to parabolic, hyperbolic and elliptic partial differential equations*, Computers & Mathematics with Applications, 19 (1990), pp. 147–161.
- [57] A. R. KROMMER AND C. W. UEBERHUBER, *Computational Integration*, SIAM, 1998.

- [58] V. I. KRYLOV AND A. H. STROUD, *Approximate Calculation of Integrals*, Courier Corporation, 2006.
- [59] L. KUIPERS AND H. NIEDERREITER, *Uniform Distribution of Sequences*, Courier Corporation, 2012.
- [60] E. LARSSON AND B. FORNBERG, *A numerical study of some radial basis function based solution methods for elliptic pdes*, *Computers & Mathematics with Applications*, 46 (2003), pp. 891–902.
- [61] E. LARSSON AND B. FORNBERG, *Theoretical and computational aspects of multivariate interpolation with increasingly flat radial basis functions*, *Computers & Mathematics with Applications*, 49 (2005), pp. 103–130.
- [62] J. B. LASSERRE, *Simple formula for integration of polynomials on a simplex*, *BIT Numerical Mathematics*, 61 (2021), pp. 523–533.
- [63] B. F. MANLY, *Bootstrap and Monte Carlo Methods in Biology*, vol. 70, CRC press, 2006.
- [64] J. C. MAXWELL, *On approximate multiple integration between limits of summation*, in *Proc. Cambridge Philos. Soc.*, vol. 3, 1877, pp. 39–47.
- [65] B. MEHRI AND S. JOKAR, *Lebesgue function for multivariate interpolation by radial basis functions*, *Applied Mathematics and Computation*, 187 (2007), pp. 306–314.
- [66] G. MIGLIORATI AND F. NOBILE, *Stable high-order randomized cubature formulae in arbitrary dimension*, arXiv preprint arXiv:1812.07761, (2018).
- [67] S. MÜLLER AND R. SCHABACK, *A Newton basis for kernel spaces*, *Journal of Approximation Theory*, 161 (2009), pp. 645–655.
- [68] K. P. MURPHY, *Machine Learning: A Probabilistic Perspective*, MIT press, 2012.
- [69] I. MYSOVSKIKH, *The approximation of multiple integrals by using interpolatory cubature formulae*, in *Quantitative Approximation*, Elsevier, 1980, pp. 217–243.
- [70] I. P. MYSOVSKIKH, *Cubature formulae that are exact for trigonometric polynomials*, TW Reports, (2001). Edited by R. Cools and H.J. Schmid.
- [71] H. NIEDERREITER, *Random Number Generation and Quasi-Monte Carlo Methods*, SIAM, 1992.
- [72] F. W. J. OLVER, A. B. OLDE DAALHUIS, D. W. LOZIER, B. I. SCHNEIDER, R. F. BOISVERT, C. W. CLARK, B. R. MILLER, B. V. SAUNDERS, H. S. COHL, AND M. A. MCCLAIN, *NIST Digital Library of Mathematical Functions*. Release 1.1.1, March 15, 2021, 2021, <http://dlmf.nist.gov/>.
- [73] M. PAZOUKI AND R. SCHABACK, *Bases for kernel-based spaces*, *Journal of Computational and Applied Mathematics*, 236 (2011), pp. 575–588.
- [74] A. PUNZI, A. SOMMARIVA, AND M. VIANELLO, *Meshless cubature over the disk using thin-plate splines*, *Journal of Computational and Applied Mathematics*, 221 (2008), pp. 430–436.
- [75] A. QUARTERONI AND A. VALLI, *Numerical Approximation of Partial Differential Equations*, vol. 23, Springer Science & Business Media, 2008.
- [76] J. A. REEGER AND B. FORNBERG, *Numerical quadrature over the surface of a sphere*, *Studies in Applied Mathematics*, 137 (2016), pp. 174–188.
- [77] J. A. REEGER AND B. FORNBERG, *Numerical quadrature over smooth surfaces with boundaries*, *Journal of Computational Physics*, 355 (2018), pp. 176–190.
- [78] J. A. REEGER, B. FORNBERG, AND M. L. WATTS, *Numerical quadrature over smooth, closed surfaces*, *Proceedings of the Royal Society A: Mathematical, Physical and Engineering Sciences*, 472 (2016), p. 20160401.
- [79] W. RUDIN, *Real and Complex Analysis*, McGraw-Hill Education, 1987.
- [80] R. SCHABACK, *Error estimates and condition numbers for radial basis function interpolation*, *Advances in Computational Mathematics*, 3 (1995), pp. 251–264.
- [81] R. SCHABACK, *Multivariate interpolation by polynomials and radial basis functions*, *Constructive Approximation*, 21 (2005), pp. 293–317.
- [82] C. SHU AND Y. WU, *Integrated radial basis functions-based differential quadrature method and its performance*, *International Journal for Numerical Methods in Fluids*, 53 (2007), pp. 969–984.
- [83] A. SOMMARIVA AND M. VIANELLO, *Meshless cubature by Green’s formula*, *Applied mathematics and computation*, 183 (2006), pp. 1098–1107.
- [84] A. SOMMARIVA AND M. VIANELLO, *Numerical cubature on scattered data by radial basis functions*, *Computing*, 76 (2006), p. 295.
- [85] A. SOMMARIVA AND M. VIANELLO, *RBF moment computation and meshless cubature on general polygonal regions*, *Applied Mathematics and Computation*, 409 (2021), p. 126375.
- [86] A. SOMMARIVA AND R. WOMERSLEY, *Integration by rbf over the sphere*, Applied Mathematics Report

- AMR05/17, University of New South Wales, (2005).
- [87] A. H. STROUD, *Approximate Calculation of Multiple Integrals*, Prentice-Hall, 1971.
  - [88] L. N. TREFETHEN, *Cubature, approximation, and isotropy in the hypercube*, SIAM Review, 59 (2017), pp. 469–491.
  - [89] L. N. TREFETHEN, *Exactness of quadrature formulas*, arXiv preprint arXiv:2101.09501, (2021).
  - [90] L. VAN DEN BOS, B. SANDERSE, AND W. BIERBOOMS, *Adaptive sampling-based quadrature rules for efficient Bayesian prediction*, Journal of Computational Physics, (2020), p. 109537.
  - [91] M. L. WATTS, *Radial basis function based quadrature over smooth surfaces*, 2016, <https://scholar.afit.edu/etd/249>. Theses and Dissertations.
  - [92] H. WENDLAND, *Piecewise polynomial, positive definite and compactly supported radial functions of minimal degree*, Advances in computational Mathematics, 4 (1995), pp. 389–396.
  - [93] H. WENDLAND, *Scattered Data Approximation*, vol. 17, Cambridge University Press, 2004.
  - [94] H. WEYL, *Über die Gleichverteilung von Zahlen mod. Eins*, Mathematische Annalen, 77 (1916), pp. 313–352.
  - [95] G. B. WRIGHT AND B. FORNBERG, *Stable computations with flat radial basis functions using vector-valued rational approximations*, Journal of Computational Physics, 331 (2017), pp. 137–156.